U.PORTO

FACULDADE DE FARMÁCIA
UNIVERSIDADE DO PORTO

Electrochemical biosensor for phenols and catecholamines based on tyrosinase immobilized on gold nanoelectrode ensembles

Ana Isabel Ribeiro de Pinho

Dissertação de Mestrado em Controlo de Qualidade,
área de especialização em Águas e Alimentos

Trabalho realizado sob a orientação da Prof. Doutora Cristina Delerue- Matos, Co-orientação da Prof.ª Doutora Maria Beatriz Oliveira e do Doutor Viswanathan Subramanian

2 Novembro 2010

Agradecimentos

À Prof.ª Beatriz por ter sido a mentora deste projecto e por me ter encaminhado para o Isep.

À Prof.ª Cristina por me ter acolhido no seu laboratório, pela disponibilidade dispensada e pelo apoio prestado.

To Dr. Viswanathan, for the long hours that spend with me and for the thoughts that transfer during this project. THANKS VERY MUCH! Without you nothing of this was possible. To meet you was a big pleasure!

Às minhas colegas de laboratório, pela preocupação, carinho e apoio que demonstraram.

À minha amiga Patrícia pelo apoio, preocupação e “divulgação” deste projecto

À minha colega de trabalho, Patrícia pelo apoio prestado.

A ti, Nuno, que sem a tua força, incentivo, compreensão e apoio este passo importante da minha vida não teria sido dado. Sem a tua força não estaria nesta fase.

Por fim, ao meus pais, que são o meu suporte. Sem vocês os sonhos não eram possíveis de se realizar. Obrigado pelo apoio ao longo de todas as etapas da minha vida e por estarem presentes em mais uma meta alcançada.

Abstract

Nanostructured materials represent new platforms for biomolecule sensing, providing increased sensitivity and facilitating miniaturization. Many arrayed nanostructures comprise electroactive materials, exhibiting improved promise for ultrasensitive biosensing relative to conventional electrochemical electrode. Among various strategies for synthesizing the nanoscopic materials reported in the literature, template synthesis is one of the most popular approaches for fabricating three-dimensional (3D) nanostructured arrays for sensor applications. Electrochemical methods are well suited for detecting organic compounds because of their simplicity and efficiency**.** Gold nanoelectrodes ensemble were prepared by using electroless deposition of the metal within the pores of polycarbonate track-etched membranes. *Tyrosinase* enzyme has been immobilized onto preformed self-assembled monolayers of mercaptoethylamine on gold nanoelectrode via cross-linking with glutaraldehyde. Flow injection analysis systems in wall-jet configurations using this tyrosinase -modified nanoelectrodes are developed. Gold nanoelectrode ensembles (GNEEs), 50 nm in diameter and 180±20 nm in length were prepared by electroless template synthesis in polycarbonate filter membranes, followed by selective controlled sequential polycarbonate dissolution using DCM/EtOH (V∶ V＝1∶3). The electrochemical evaluation of the 3D GNEEs was conducted using the well known $[Fe(CN)_6]^{3-}$/$[Fe(CN)_6]^{4-}$ couple. Compared with 2D GNEEs, the 3D GNEEs significantly enhanced the current response in cyclic voltammetry. The electrochemical results demonstrated the fact that electron transfer process could be effectively improved at the 3D cylindrical GNEEs. Linear diffusion is dominant on the cylindrical GNEEs at conventional scan rates. Under optimized conditions, high reproducible results were obtained, linear calibration was achieved in the $1x10^{-6}$ M to $1x10^{-3}$ M concentration range and the detection limit was $1x10^{-8}$ M. Moreover, negligible interferences from species like 100 mM glucose, 20 mM ascorbic acid and 100 mM urea were observed at a potential of -0.100 V (vs. Ag/AgCl). L-dopa and dopamine spiked serum samples were analyzed for recovery studies.

Keywords: Nanostructured materials; Gold nanoelectrode ensembles; Electroless deposition; Enzyme; Flow injection analysis

Resumo

Os nanomateriais representam novas plataformas, para a detecção de biomoléculas, uma vez que proporcionam maior sensibilidade e são de fácil miniaturização. Estes nanomateriais usados em biossensores ultra-sensíveis englobam, na sua maioria, materiais electroactivos, em que o seu uso tem mostrado ser um sucesso, quando comparados com os eléctrodos convencionais. Entre os vários métodos apresentados na literatura, para sintetizar os nanomaterias, o método "*template*" é um dos métodos mais usados na fabricação de nanoestruturas tridimensionais (3D). Os métodos electroquímicos, devido à sua simplicidade e eficiência, são várias vezes usados para detecção de compostos orgânicos.

Os nanoeléctrodos de ouro foram preparados por deposição química em que o metal se deposita nos poros das membranas de policarbonato. A enzima *Tirosinase* foi imobilizada, em monocamadas organizadas e pré-formadas de mercaptoetilamina sob os nanoeléctrodos de ouro, usando o glutaraldeído como agente reticular**.** Foram desenvolvidos sistemas de fluxo contínuo usando os nanoeléctrodos de ouro modificados com Tirosinase. Os nanoeléctrodos de ouro, com 50 nm de diâmetro e 180±20 nm de comprimento foram preparados pelo método " *template*", deposição química do metal nas membranas de policarbonato, seguindo-se a dissolução sequencial da membrana, usando DCM/EtOH (V:V;1:3). A análise electroquímica dos nanoeléctrodos de ouro 3D, realizou-se com o conhecido par $[Fe(CN)_6]^{3-}/[Fe(CN)_6]^{4-}$. Quando comparados os sinais obtidos por voltametria cíclica, com os nanoeléctrodos de ouro de 2D e 3D, constata-se que há um aumento considerável da intensidade de corrente no que diz respeitos aos eléctrodos 3D. Os resultados electroquímicos mostram que o processo de transferência de electrões pode ser melhorado para o caso dos nanoeléctrodos de ouro cilíndricos a 3D. A difusão linear é dominante para o caso dos nanoeléctrodos de ouro cilíndricos, para velocidades de varrimento convencionais. Após optimização de todos os parâmetros experimentais, os resultados apresentam elevada reprodutibilidade, para o intervalo de calibração linear entre $1x10^{-6}$ M e $1x10^{-3}$ M, obtendo-se um limite de detecção de $1x10^{-8}$ M. O estudo de interferências foi realizado a um potencial de -0,100 V (vs. Ag/AgCl) para 100 mM de glucose, 20 mM de ácido ascórbico e 100 mM de ureia, tendo-se verificado não serem significativas. Para os estudos de recuperação, amostras de soro fisiológico foram contaminadas com L-dopa e dopamina.

Palavras-chave: Nanomateriais, nanoelectrodos de ouro, deposição química, enzima, sistema de fluxo contínuo

Index

Index of Figures

Index of Schemes

Index of Table

Abbreviations

DA	Dopamine
DOPAC	3,4-dihydroxyphenylacetic acid
L-dopa	Levedopa
Ag	Antigene
Ab	Antibody
DNA	Deoxyribonucleic acid
EIAs	Enzyme immunoassays
HRP	Horseradish peroxidase
ALP	Alkaline phosphatase
GOD	Glucose oxidase
Z	Impedance
R	Resistance
C	Capacitance
O_2	Oxygen
H_2O_2	Hydrogen peroxide
SAMs	Self assembled monolayers
NADH	Nicotinamide adenine dinucleotide
ZnO	Zinc oxide
BLMs	Bi-layer lipid membranes
PVC	Polyvinyl chloride
1D	One-dimensional
CNT	Carbon nanotubes
SWCNT	Single- walled carbon nanotubes
NEAs	Nanoelectrode arrays
NEEs	Nanoelectrode ensembles
PPy	Polypirrole

$HAuCl_4$	Chloroauric acid
GCE	Glassy electrode carbon
GNEEs	Gold nanoelectrode ensembles
2D	Two-dimensional
3D	Three-dimensional
FIA	Flow injection analysis
D	Dispersion coefficient
C^0	Concentration of a pure dye
C^{max}	Concentration of injected dye as it passes through the detector
C	Measured concentration of the injection
R	Reagent
S	Sample
h	height
W	Width
A	Area
T	Residence time
tb	Peak width at the baseline
PPOs	Polyphenoloxidases
Au-S	Gold-sulfur
DOPA	3-(3,4-dihydroxyphenyl) alanine
SEM	Scanning electron micrographs
PCTE	Polycarbonate Track-etched membranes
PBS	Phosphate buffered saline
TFA	Trifluoroacetic acid
Au	Gold
DMC	Dichloromethane

EtOH	Ethanol
GA	Glutaraldehyde
EDX	Energy dispersive X-ray
$[Fe(CN)_6]^{3-}$	Ferricyanide
ΔE_{pk}	Peak separation
I_{pc}	Cathodic peak
v	Scan rate
NH_2	Amino
TyrE	Tyrosinase enzyme
LOD	Limit of detection

1.Introduction

1.1 Introduction

Quantification of extracellular levels of neurotransmitters in the brain with a high degree of quality and reliability has been a fundamental challenge for analytical chemists for years. With the ability to characterize how neurotransmitter levels change in response to the administration of different pharmacological agents, it is possible to learn about the mechanisms by which drugs elicit their effect. Characterizing neurotransmitter levels in diseased states enables mapping of a disease or treatment, and may guide the development of novel therapies.

1.2 Neurotransmitters

Neurotransmitters are brain chemicals that communicate information throughout the brain and body, relaying signals between neurons. Catecholamines originate from a wide range of neural pathways by employing biogenic amines as neurotransmitters [1]. The neurotransmitter metabolites released into the cerebrospinal fluid can be a sensitive indicator of neuronal functioning in nearby diencephalon structures [2]. Therefore, it is of great clinical importance to measure neurotransmitters and their metabolites level in the extracellular fluid in order to monitor neurotransmission process [3] (Fig.1.1). Functioning in dynamic balance are two kinds of neurotransmitters: the excitatory (such as nor-epinephrine), which stimulate, and the inhibitory (such as serotonin), which calm the brain to balance mood.

Dopamine (DA), which is the most important neurotransmitter among the catecholamines, plays an important role in the function of central nervous, renal, hormonal and cardiovascular systems. DA has also been associated with the reward system; the circuitry in the brain is responsible for the motivation to seek out stimuli as well as the emotions for feeling satisfied and satiated in one's environment [4]. From the view of point of physiological importance, it is a challenge to monitor DA and its metabolite of 3,4-dihydroxyphenylacetic acid (DOPAC), because DA level control is vital in the treatment of Parkinson's disease. Levodopa (L-dopa) is the medication of choice for the treatment of Parkinson's disease, which is principally metabolized by L-dopa decarboxylase to dopamine, compensating for the deficiency of dopamine in the brain.

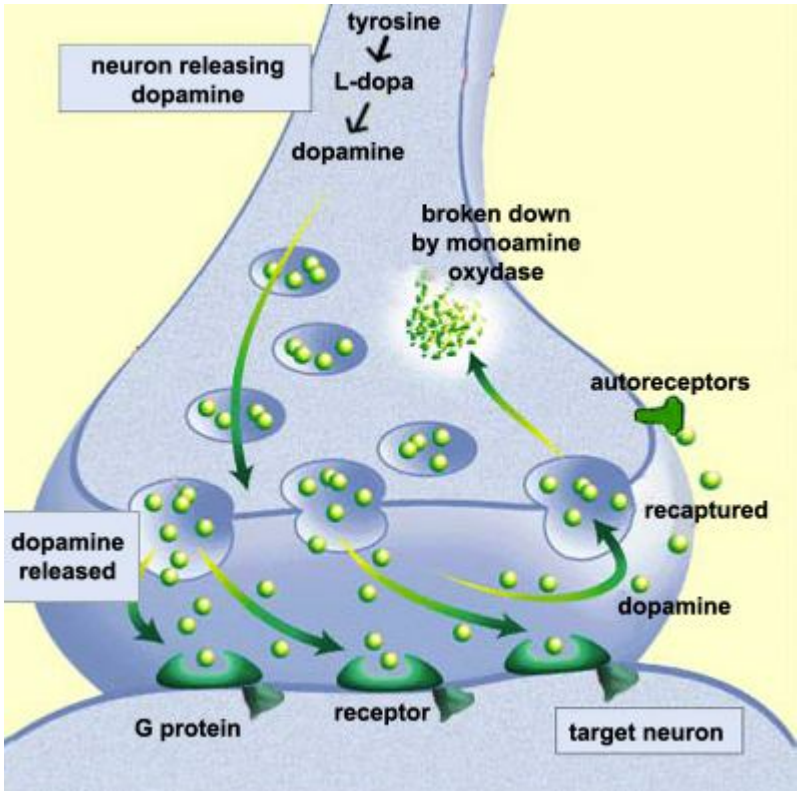

Figure 1.1 Structure of a typical chemical synapse

The analysis of neurotransmitters is of substantial interest for the rapid and early detection of neural disorders. Several electrochemical and optical methods for the analysis of neurotransmitters are available in recent literature. Other reports have addressed the analysis of neurotransmitters by capillary electrophoresis and by mass spectrometry. These conventional techniques are expensive, complicated and slow, whereas virtually inexhaustible development opportunity and immense market potential are giving the development of biosensor an edge over the others. Electrochemical techniques care an attractive method for the determination of DA because of their high sensitivity as well as their applicability to real-time detection of DA in brain tissues. Tyrosinase based electrochemical biosensor is a promising and effective tool for the determination of neurotransmitters such as DA and L-Dopa.

1.3 Biosensor

Biosensor-related research has shown tremendous growth over the last two decades. A biosensor is generally defined as an analytical device which converts a biological

response into a quantifiable and processable signal [5]. The general scheme of amperometric biosensors is shown in Fig.1.2. The interaction of the analyte with the bioreceptor is designed to produce an effect measured by the transducer, which converts the information into a measurable effect, for example, an electrical signal.

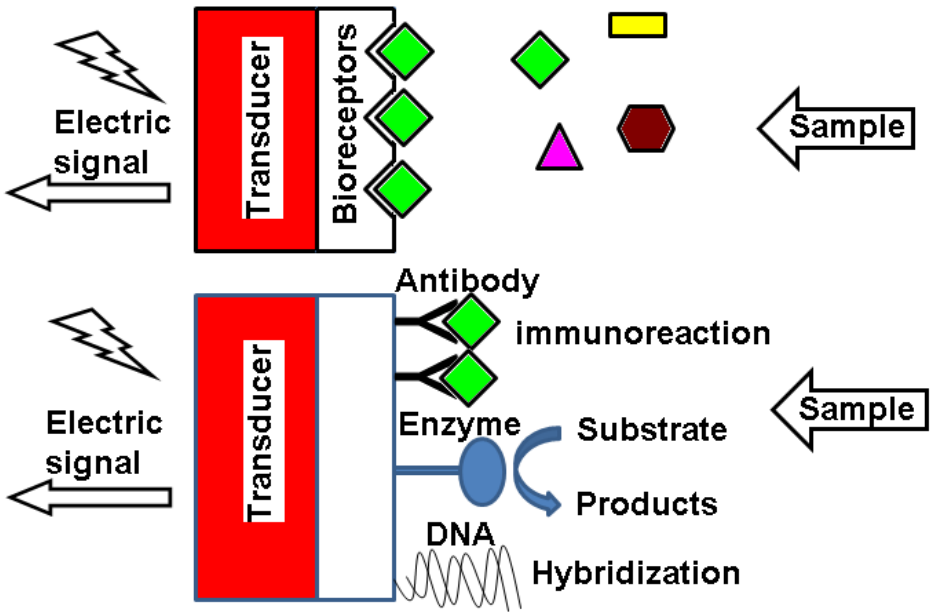

Figure 1.2 The general scheme of amperometric biosensors

Biosensors can be applied to a large variety of samples including body fluids, food samples, cell cultures and be used to analyze environmental samples. Designed for the purpose, biosensors are generally highly selective due to the possibility to tailor the specific interaction of compounds by immobilizing biological recognition elements on the sensor substrate that have a specific binding affinity to the desired molecule [6]. Typical recognition elements used in biosensors are: enzymes, nucleic acids, antibodies, whole cells, and receptors. Of these, enzymes are among the most common [7]. To fully exploit the specific interaction through biorecognition, the surface architecture of the sensor also must suppress any non-specific interaction. A tremendous research effort has been invested to find surface modifications with specific interaction capabilities over prolonged periods of time in biological fluids [8]. In particular, the ability to tailor the size and

structure and hence the properties of nanomaterials offers excellent prospects for designing novel sensing systems and enhancing the performance of the bioanalytical assay [8, 9]. Intense efforts have been devoted to the development of so-called second- and third generation biosensors [10].

1.3.1 Classifications of Biosensor

From the definition of biosensors, they can be classified either by their biological recognition element or their signal transduction mechanism. However, additional biosensor features could be analyzed.

1.3.2 Classification based on bioreceptors

Recent developments in biosensors research have centred on bioreceptors with improved biosensor design. Bioreceptors are used because they are important elements to specificity for biosensor technologies. They are biological molecular species (e.g., an antibody, an enzyme, a protein, or a nucleic acid) or a living biological system (e.g., cells, tissue, or whole organisms) that utilizes a biochemical mechanism for recognition. They allow binding the specific analyte of interest to the sensor for the measurement with minimum interference from other components in complex mixtures. According to bio receptor, biosensors can be classified into the following categories such as enzymatic biosensors, immunosensor, DNA (Deoxyribonucleic acid) biosensors, aptasensors and cells based biosensors etc.

1.3.2.1 Enzymatic biosensors

This class of biosensors employs enzymes as biocatalysts. Enzymes react with the analyte or the substrate producing a detectable signal through this biorecognition process [11]. An example of these types of biosensors is the use of an enzyme acting specifically to convert a reactant molecule into a product. Some enzymes show a specific sensitivity to a particular molecule (or substrate). Many enzymatic reactions involve cofactors. These cofactors are other molecules or ions that assist in the reaction. During the catalysis, the cofactors may be chemically changed, and as a consequence, the resulting physicochemical effects can monitor or detect the enzymatic process. The most famous

practical device for determination of blood glucose content is an enzymatic biosensor and it was developed by Yellow Springs Instruments in the early 1970s [12].

1.3.2.2 Immunosensors

Immunosensors are based on the antibody-antigen interaction and the transduction of the biorecognition event into a physical signal. The antigen is recognized as a foreign body. A specific antibody is generated to act against it by binding to it and operating to remove the antigen. By this specific recognition and interaction performed on the molecular level, antibodies and antigens can be exploited as a means for diagnostic testing. Antibodies can be raised in vitro to detect specific molecules. In this way, antibodies may serve as the basis for the biosensor detection system. The binding of an antigen (Ag) to the appropriate antibody (Ab) is accompanied by only small physicochemical changes. Lack of sufficient sensitivity for detecting analytes at low concentrations is a major impediment to development of label-free immunosensors. The utility of biosensing immunosensors would be greater if there was a proper strategy to amplify the immunological interactions so as to result in more pronounced changes [13]. The design and preparation of an optimum interface between the biological element and the detector material is the key part for this kind of sensors [14].

1.3.2.3 Enzyme immunoassays

Enzyme immunoassays (EIAs) based on electrochemical detection offer several potential advantages and have been applied in clinical, medical, biotechnological, food and environmental analysis. Among the enzyme labels employed, horseradish peroxidase (HRP), alkaline phosphatase (ALP) and glucose oxidase (GOD) are the most common. Recently, Ricci et al. [15] reviewed about recent advances, challenges, and trends of electrochemical EIAs focusing on HRP, ALP or GOD as labels over the past five years. Recently, label-free electrochemical immunoassay for detection of proteins has become an important topic in bioanalysis [16].

1.3.2.4 DNA based biosensors

DNA biosensors are commonly employed to detect specific sequences of DNA. They can reach high levels of selectivity and affinity based on the hybridization between a DNA.

Each type of cell has within it a unique signature in its DNA. All of the information contained in the DNA appears encoded in a series of amino acids and, as such, forms the identifying backbone of that structure. The recognition of these sequences is of fundamental importance to the control, reading, and detection of these molecular structures. The basic principle of a DNA biosensor is to detect the molecular recognition provided by the DNA probes and to transform it into the signal using a transducer.

1.3.2.5 Aptasensors

Aptamers are artificial nucleic acid ligands that can be generated against amino acids, drugs, proteins and other molecules. They are isolated from combinatorial libraries of synthetic nucleic acid by an iterative process of adsorption, recovery and reamplification. Aptamers, first reported in 1990, are attracting interest in the areas of therapeutics and diagnostics and offer themselves as ideal candidates for use as biocomponents in biosensors (aptasensors), possessing many advantages over state of the art affinity sensors. In general, aptamers are small (i.e., 40 to 100 bases), synthetic oligonucleotides that can specifically recognize and bind to virtually any kind of target, including ions, whole cells, drugs, toxins, low-molecular-weight ligands, peptides, and proteins. Aptamers can function as the biorecognition elements in biosensor applications [17]. Aptamers can be defined as in *vitro* selected functional oligonucleotides that bind a specific target molecule. Due to their inherent selectivity, affinity, and their advantages over traditional recognition elements, they represent an interesting alternative for biosensing. Aptamers are small in size in comparison to other biorecognition molecules such as antibodies, protein and enzymes. This allows efficient immobilization at high density. Therefore, production, miniaturization, integration, and automation of biosensors can be accomplished more easily with aptamers than with antibodies [18]. As for the protein-based biosensors, the significant conformational change of most aptamers upon target binding offers great flexibility in the design of biosensors.

1.3.2.6 Whole-Cells or Organelles based biosensors

Whole-cell bacterial biosensors are bacteria engineered to recognize a specific analyte. The signal-transduction is performed by the production of an easily quantifiable marker protein. In most cases, an existing regulatory system in the bacterial cell is exploited to

drive expression of a specific reporter gene, such as bacterial green fluorescent protein, beta-galactosidase and others [19].

1.3.3 Classification based on the transduction method

The advances in transduction are closely linked to the accelerated technological breakthroughs related to electronics, informatics, data mining, and computer technologies. Signal transduction and data analysis research, oriented to lowering the cost and portability of biosensor analysis, are areas of high activity in electrical and electronic engineering, and analytical chemistry and lead in accelerated pace to more reliable and easy to use biosensors. Biosensor technologies include transduction platforms based on four major types of transducers: electrochemical (electrodes), optical (optrodes), mass (piezoelectric crystals or surface acoustic wave devices), and thermal (thermistors or heat-sensitive sensors). These techniques have been adapted to detect analytes of interest based on the interaction with or functionality modification of biological targets. The specificity of the detection is determined by the biological component of the method.

1.3.3.1 Electrochemical Transducers

The biochemical signals can be used to generate a current/charge or may change conductivity between two electrodes. The corresponding transduction device can be described as potentiometric, amperometric and conductometric/impedimetric. Demands of high sensitivity, specificity, rapid analysis with accuracy of the analytical measurements have brought considerable thrust in the developing electrochemical biosensor as novel diagnostic tools in technology [20].

1.3.3.2 Optical Transducers

These have taken a new lease of life with the development of fibre optics, thus allowing greater flexibility and miniaturization. The techniques used include absorption spectroscopy, fluorescence spectroscopy, luminescence spectroscopy, internal reflection spectroscopy, surface plasmon spectroscopy and light scattering etc.

1.3.3.3 Electrical Transducers: Filed Effect Transistor based sensors

Miniaturization can sometimes be achieved by constructing one of the above types of electrochemical transducers on a silicon chip- based field-effect transistor.

1.3.3.4 Piezo-Electric Sensors

These devices involve the generation of electric currents from a vibrating crystal. The frequency of vibration is affected by the mass of material adsorbed on its surface, which could be related to changes in a reaction. Surjiuce acoustic wave devices are a related system.

1.3.3.5 Thermal Sensors

All chemical and biochemical processes involve the production or absorption of heat. This heat can be measured by sensitive thermistors and hence be related to the amount of substance to be analysed.

1.4 Electrochemical Biosensors

Among the various types of biosensors, the electrochemical biosensors are the most common as a result of numerous advances leading to their well understood biointeraction and detection process.

1.4.1 Classifications of electrochemical biosensors

The basic principle of electrochemical sensors is that the electroactive analyte is undergoes oxidized or reduced on the working electrode surface which is subjected to some predefined pattern of fixed or varying potential, and the variation on electron fluxes leads to the generation of an electrochemical signal, which is measured by the electrochemical detector. The two most important subclasses of electrochemical sensors include the voltammetric and potentiometric biosensors.

1.4.1.1 Voltammetric sensors

Voltammetric sensors investigate the concentration effect of the detecting species on the current potential characteristics of the reduction or oxidation of a specific reaction [21]. Amperometric sensors are a subclass of the voltammetric sensors. The principle of functioning for the amperometric sensors is based on the application of a fixed potential to the electrochemical cell, resulting in a current because of an oxidation or reduction reaction. The current is, then, used to quantify the species involved in the reaction [22, 23]. The versatility of amperometric biosensors is also apparent from their direct or indirect measurement capability. As Chaubey and Malhotra [24] describes, direct amperometry makes use of the intimate relationship between the products of the redox reaction and the measured current, whereas indirect amperometry uses conventional detectors to measure the metabolic substrate or product of the analyte of interest [25]. The amperometric biosensors are often used on a large scale for analytes such as glucose, lactate [26, 27], and sialic acid [28, 29].

1.4.1.2 Potentiometric biosensors

Potentiometric biosensors examine the potential difference measurement between the working electrode and the reference electrode as it relates to the redox reaction of the species of interest. The potentiometric biosensors monitor the accumulation of charge at zero current created by selective binding at the electrode surface [30]. A disadvantage of these sensors compared with the amperometric counterparts is the extended time period required for the potentiometric sensor to reach equilibrium required for data collection.

1.4.1.3 Impedimetric biosensors

Such devices follow either impedance (Z) or its components resistance (R) and capacitance (C); inductance typically has only a minimal influence in a typical electrochemical setup. Thus, the expression of impedance is as follows:

$$Z^2 = R^2 + \frac{1}{(2fC)^2}$$

The inverse value of resistance is called conductance and for this reason some investigators name such systems as conductometric. Impedance biosensors include two electrodes with applied alternating voltage; amplitudes from a few to 100 mV are used. The impedance biosensor is commonly a functional part of the Wheatstone bridge. The enzymatically produced ions are able to provide a significant increase of impedance. Alternatively, impedance biosensors have been successfully used for microorganism growth monitoring due to the production of conductive metabolites [31, 32]. False positive results due to electrolytes from the samples are the main disadvantage of impedance biosensors. Impedimetric biosensors are less frequent compared to potentiometric and amperometric biosensors; nevertheless, there have been some promising approaches. Hybridization of DNA fragments previously amplified by a polymerase chain reaction has been monitored by an impedance assay [33]. A model impedance immunosensor containing electrodeposited polypyrrole film with captured avidin connected through biotin to anti-human IgG was able to detect antibodies as low as 10 pg/mL present in a sample [34].

1.4.1.4 Enzyme based electrochemical biosensors

Enzyme is a biological catalyst with extremely high specificity and efficacy. It must be remembered that a catalyst permit to reach easily the equilibrium without modifying its position. However, most of the enzymatic reactions take place in a short time at normal temperature, without using dramatic value of pressure and pH, and work at much higher rates in comparison to the common chemical organic and inorganic catalysts. Enzyme-catalyzed reactions are normally from 10^3 to 10^7 faster than the same noncatalyzed reactions. They are extremely specific and selective for the substrate which they interact with. Enzymes generally have a variable specificity degree, catalysing either a group of substrates that have correlated structures or a single molecule. Some kind of them assesses a good degree of stereo-specificity, as they catalyze only one of two substrate stereoisomer. The foremost general feature of enzymes is the reaction specificity. In fact they do not generate useless by-products of the reaction and give as high yield in the enzymatic reactions as almost 100%.Enzymes are generally bigger than the substrate they bind, so that only a little portion of substrate is effectively involved in the enzymatic reaction. The molecular recognition of the substrate is achieved by the well known *lock and key* principle between the respective receptor area and the analyte to be recognized.

1.4.2 Amperometric enzyme sensors

Three different styles of amperometric enzyme sensors have been developed over the last 50 years. They are often referred to as first-, second-, and third-generation amperometric enzyme sensors (Fig. 3). They all require the enzymes be in close proximity to the electrode surface, but differ in the mechanism by which signal transduction occurs.

1.4.2.1 First generation amperometric enzyme sensors

First generation amperometric enzyme sensors were first proposed by Clark and Lyons in 1962[35], and later implemented by Updike and Hicks in 1967 [36]. Updike and Hicks coined the term enzyme sensors [35]. These sensors possess oxidase enzymes in close proximity to the electrode surface, which, upon interacting with substrate, consume oxygen (O_2) and produce hydrogen peroxide (H_2O_2) (Fig. 1.3). Because O_2 and H_2O_2 are electroactive and diffusible, the amount of O_2 consumed or H_2O_2 produced by the reaction of the oxidase enzyme with substrate is used as a measure of substrate present [35-37].

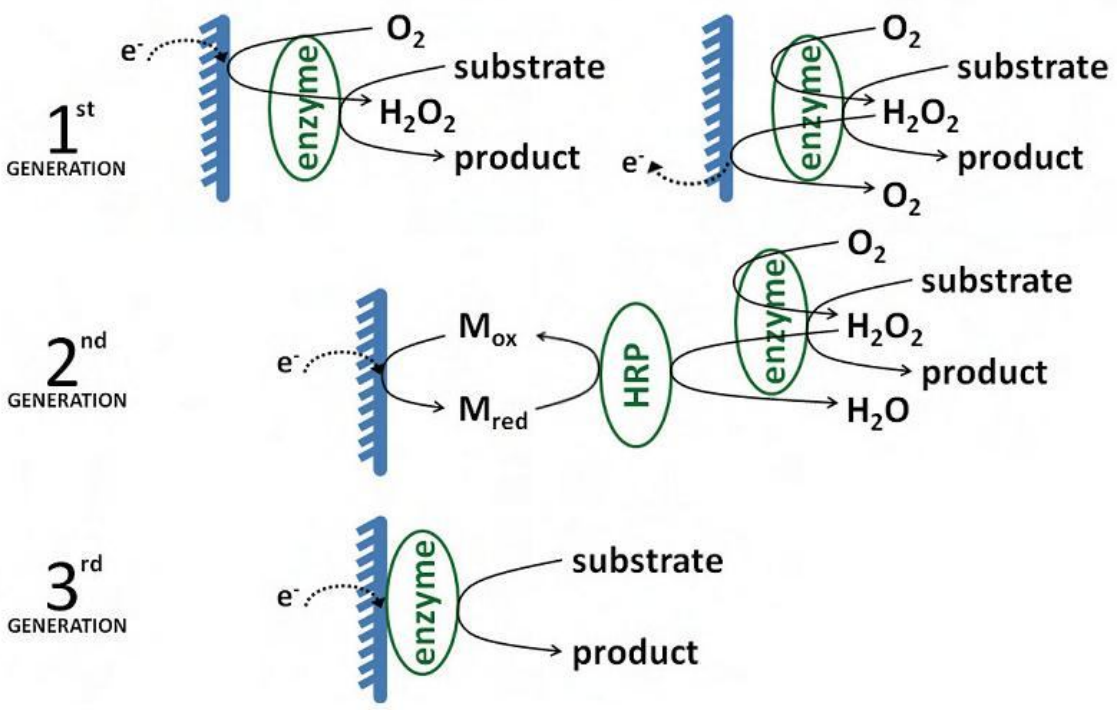

Figure 1.3 Scheme of different generations of amperometric enzyme sensors

1.4.2.2 Second generation amperometric enzyme sensors

Second generation sensors also rely on a mediated electron-transfer mechanism for signal transduction to occur. These sensors typically incorporate horseradish peroxidase (HRP) and an oxidase enzyme to oxidize the substrate. These sensors operate on the principle that H_2O_2 is produced from the reaction of the oxidase enzyme with substrate, and HRP, an oxidoreductase, can both reduce H_2O_2 , and oxidize a mediator to initiate the electron transfer process (Fig. 1.3). The amount of oxidized mediator detected amperometrically at the electrode is used as a measure of the amount of substrate present. Redox mediators may be diffusible or non-diffusible [38- 41]. In the case that mediators are diffusible, some redox equivalents may be lost to diffusion, (i.e., diffuse out of the sensor and never be detected at the electrode). Because a loss of redox equivalents corresponds to 'lost signal', polymeric hydrogels that incorporate non-diffusible redox components have been prepared. The non-diffusible redox mediators utilize an electron hopping mechanism to facilitate electron transfer between redox sites. This prevents a loss of redox equivalents because electrons will hop from one redox site to another until they are detected at the electrode surface.

1.4.2.3 Third generation amperometric enzyme sensors

Third generation enzyme sensors rely on a direct, rather than mediated, electron transfer mechanism. The amperometric current measured is the result of oxidation or reduction of the enzyme's prosthetic group, which serves as temporary trap of electrons or electron vacancies (Fig. 1.3). Third generation enzyme sensors frequently use self assembled monolayers (SAMs) to align the enzymes in a proper orientation, and connect the enzymes' prosthetic groups to the electrode. As explained by Marcus theory, electron transfer decays exponentially with distance; hence, minimizing the distance between the enzymes' prosthetic groups and the electrode is essential for the success of these sensors. In the event that an oxidase enzyme is attached to the self-assembled monolayer, electron transfer is not affected by the amount of O_2 present. O_2 must be present to withdraw electrons from oxidase enzymes in first and second generation amperometric enzyme sensors. However, in the case of third generation enzyme sensors, this can be accomplished by controlling the voltage applied to the electrode. The choice of the sensing electrode depends primarily upon the enzymatic system employed. Amperometric probes are highly suitable when oxidase or dehydrogenase enzymes,

generating electro-oxidizable peroxide or nicotinamide adenine dinucleotide (NADH) species, are employed.

1.5 Enzyme immobilization methods

The success of an enzyme biosensor ultimately relies on how well the enzyme bonds to the sensor surface and remains there during use. Immobilization between matrix and bioreceptor has been showed as the topical procedure for improving the enzyme stability and thus general biosensor performances. On the following sections different physical and chemical methods to immobilize the enzyme onto the electrode is discussed.

In order to make a viable biosensor, the biological component has to be properly attached to the transducer with maintained enzyme activity. This process is known as enzyme immobilization. Biosensors are usually designed with high enzyme loading to insure sufficient biocatalyst activities, and the enzymes are provided with an appropriate environment to sustain their activities. The local chemical and thermal environment can have profound effects on the enzyme stability. The choice of immobilization method depends on many factors, such as the nature of the biological element, the type of transducer used, the physicochemical properties of the analyte and the operating conditions in which the biosensor is to function, and overriding all these considerations is necessary for the biological element to exhibit maximum activity in its immobilized microenvironment [42]. Generally, there are four regular methods for enzyme immobilization and they are briefly described as described below (Table 1.1).

Table 1.1. Enzyme immobilization methods

Adsorption		• Simple procedure and lower costs • Based on surface activity, Vander Waals forces, ionic and hydrogen bonds, although sometimes hydrophobic bonding and combinations of above. • Poor stability
Covalent Bonding		• Functional groups involved NH_2, OH and Tyrosyl. • Stability in wide pH, ionic strength, solvent, temperature and uncontrolled conditions •Denaturation or activty loss
Cross-Linking	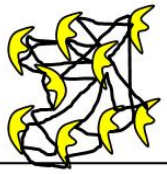	•Enzyme-enzyme bond stronger, •High loading of enzyme. •Formation of diffusion barriers
Entrapment	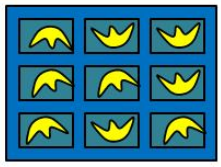	• Suit almost all types of enzymes •High loading of enzyme. • Restricted by the phenomena of steric hindrance and diffusion through the gel or membrane.

1.5.1 Adsorption

It is the simplest and fastest way to prepare immobilized enzymes. Adsorption can roughly be divided into two classes: physical adsorption and chemical adsorption. Physical adsorption is weak and occurs mainly via Vander Waals forces, ionic and hydrogen bonds, although sometimes hydrophobic bonding can become significant. These forces are weak, but sufficiently large in number to enable reasonable binding. Chemical adsorption is stronger and involves the formation of covalent bonds. Many substances adsorb enzymes on their surfaces, eg. alumina, charcoal, clay, cellulose, kaolin, silica gel, glass and collagen. Physical adsorption is mostly used for enzyme immobilization in ZnO-based glucose biosensors [43].

1.5.2 Entrapment

It refers to mixture of the biomaterial with monomer solution and then polymerised to a gel, trapping the biomaterial. However, this method can give rise to barriers to the diffusion of substrate, leading to the reaction delay. Besides, loss of bioactivity may occur

through pores in the gel. The gels commonly used include polyacrylamide, starch gels, nylon, silastic gels, conducting polymers, etc.

It is possible to distinguish between three general methods:

(i)- Entrapment behind a membrane**:** a solution or suspension of enzymes, cells, a slice of tissue is confined by an analyte permeable membrane as a thin film covering the detector;

(ii)- Entrapment of biological receptors within self assembled monolayers (SAMs) or bi-layer lipid membranes (BLMs);

(iii)- Entrapment of biomolecules within a polymeric matrix membranes (such as polyacrylonitrile, agar gel, polyurethane, or polyvinyl-alcohol), redox gels, sol-gels with redox centres [44].

1.5.3 Covalent bonding

In this method, the bond occurs between a functional group in the biomaterial to the support matrix. Some functional groups which are not essential for the catalytic activity of an enzyme can be covalently bonded to the support matrix. It requires mild conditions under which reactions are performed, such as low temperature, low ionic strength and pH in the physiological range.

1.5.4 Cross-linking

For this method, usually, biomaterial is chemically bonded to solid supports or to another supporting material such as cross-linking agent to significantly increase the attachment. It is a useful method to stabilize adsorbed biomaterials. Glutaraldehyde is the mostly used bifunctional agent. The agents can also interfere with the enzyme activity, especially at higher concentrations. Crosslinking is rarely used alone ass technique of immobilization, because the absence of mechanical properties and poor stability are severe limitations for biosensor development. This one is often used to enhance other methods of immobilization, normally in order to reduce cell leakage in other systems.

The immobilization of the receptor molecule on the sensor surface is a key point for the final performance of the sensor. The immobilization procedure must be stable and reproducible, and must retain the stability and activity of the receptor. One of the most promising strategies is immobilization based on nanotechnology. Nature of biosensing surface is very important namely the prolonged use of the sensor and an anticipated extended storage and working stability.

1.6 Importance of working electrode

In electrochemical sensing, choice of working electrode material is fundamental to the success of electrochemical measurement. In recent years solid electrodes of gold, platinum, silver, nickel, copper, various doped or undoped forms of carbon, dimensionally stable anions, etc. have replaced the conventional mercury electrodes, on the ground of toxicity. These materials can be either bare or chemically modified for improved selectivity, sensitivity and stability [45], mostly by using polymers of varied characteristics. Miniaturization of electrodes, as proposed by Wightman for the first time [46], with the advancement of micromachining, photolithography, microcontact printing, etc. has led to the development of microelectrodes (<2 mm dimension), and has opened the horizon of in vivo and in vitro applicability of electrochemical sensor systems requiring only microliter volumes of analyte and reagent [47]. But the demand for a low-cost, disposable, biosensor strips or sticks for easy commercialization was realized with recent technologies such as screen-printed electrodes [48, 49], which involves deposition of electrode material, mainly carbon and noble metals, on inert PVC or ceramic backing. Cheap, miniaturized, easy-to-use, disposable chips for electrochemical analysis of bio-analytes are very essential and many groups are working in this direction [50].

1.7 Role of nanotechnology in biosensors developments

Nanotechnology involves the study, manipulation, creation and use of materials, devices and systems typically with dimensions smaller than 100 nm. Nanotechnology is playing an increasingly important role in the development of biosensors [51, 52, 53]. Sensitivity and other attributes of biosensors can be improved by using nanomaterials in their construction. Nanomaterials, or matrices with at least one of their dimensions ranging in scale from 1 to 100 nm, display unique physical and chemical features because of effects such as the quantum size effect, mini size effect, surface effect and macro-quantum

tunnel effect. Use of nanomaterials in biosensors allows the use of many new signal transduction technologies in their manufacture. Because of their submicron size, nanosensors, nanoprobes and other nanosystems are revolutionizing the fields of chemical and biological analysis, to enable rapid analysis of multiple substances in vivo analysis.

1.7.1 Nanotechnology in electrochemical biosensors

Nanotechnology brings new possibilities for biosensor construction and for developing novel electrochemical bioassays. Nanoscale materials have been used to achieve direct wiring of enzymes to electrode surface, to promote electrochemical reaction, to impose barcode for biomaterials and to amplify signal of biorecognition event. The resulting electrochemical nanobiosensors have been applied in areas of cancer diagnostics and detection of infectious organisms. Nanomaterials, an emerging sub-discipline in chemistry has enabled the development of ultrasensitive electrochemical biosensors due to their high surface area, favourable electronic properties and electrocatalytic activity as well as good biocompatibility induced by nanometer size and specific physicochemical characteristics.

The sampling component of a biosensor contains a bio-sensitive layer that can either contain bioreceptors or be made of bio-receptors covalently attached to the transducer. For biosensing purposes, a layer of receptor molecules that are capable of binding the analyte molecules in a selective way must be previously immobilized on the transducer surface. The immobilization of the receptor molecule on the sensor surface is a key point for the final performance of the sensor. The immobilization procedure must be stable and reproducible, and must retain the stability and activity of the receptor. One of the most promising strategies is immobilization based on nanotechnology [54, 55]. It is essential to create a biosensing surface in which the sensing mechanism is immobilized. The biosensing surface may contain enzymes, antibodies, antigens, microorganisms, mammalian cells, tissues, or receptors. Nature of biosensing surface is very important namely the prolonged use of the sensor and an anticipated extended storage and working stability.

One-dimensional (1-D) nanostructures, such as carbon nanotubes (CNT) and semiconductor- or conducting polymer nanowires, are particularly attractive materials for working electrode in biosensors. Because of the high surface-to-volume ratio and novel electron transport properties of these nanostructures, their electronic conductance is strongly influenced by minor surface perturbations (such as those associated with the binding of macromolecules). Such 1-D materials thus offer the prospect of rapid (real time) and sensitive label-free bioelectronic detection, and massive redundancy in nanosensor arrays. These nanomaterials would allow packing a huge number of sensing elements onto a small footprint of an array device. The remarkable properties of CNT suggest the possibility of developing superior electrochemical sensing devices, ranging from amperometric enzyme electrodes to label-free DNA hybridization biosensors [55]. An extremely important challenge in amperometric enzyme electrodes is the establishment of satisfactory electrical communication between the active site of the enzyme and the electrode surface. The redox center of most oxidoreductases is electrically insulated by a protein shell. Because of this shell, the enzyme cannot be oxidized or reduced at an electrode at any potential. The possibility of direct electron-transfer between enzymes and electrode surfaces could pave the way for superior reagentless biosensing devices, as it obviates the need for co-substrates or mediators and allows efficient transduction of the biorecognition event. ‘‘Trees’’ of aligned CNT in the nanoforest, prepared by self assembly, can act as molecular wires to allow electrical communication between the underlying electrode and redox proteins which is covalently attached to the ends of the single- walled carbon nanotubes (SWCNT) [56,57] . Willner’s group demonstrated that aligned reconstituted glucose oxidase (GOD) on the edge of SWCNT can be linked to an electrode surface [58]. Such enzyme reconstitution on the end of CNT represents an extremely efficient approach for ‘plugging’ an electrode into GOD. Arrays of nanoscopic gold tubes or wires have been prepared by electroless deposition of the metal within the pores of polycarbonate particle track-etched membranes [59]. Glucose oxidase was immobilized onto the preformed self-assembled monolayers (SAMs) (mercaptoethylamine or mercaptopropionic acid) of gold tubes, via cross-linking with glutaraldehyde or covalent attachment by carbodiimide coupling. Glucose responses as large as 400 nA /mM cm^2 were obtained. Based on a slimier method of template synthesis,[60] immobilized glucose oxidase in the polypyrrole nanotubes and produced a biosensor. Compared to conventional biosensor, immobilization on nanomaterials enhanced the amount of the enzyme loading, the retention of the immobilized activity and the sensitivity of the biosensor [9].

1.7.2 Nanoarrays, nanotubes, nanoparticules electrodes

Nano-structured materials have proven as one of the most powerful tool in new technologies and research, due to their absolutely peculiar properties at nanometer size scale. Many studies have shown that optical, mechanical, photo-catalytic and transport properties drastically changes, depending on quantum size effect, as the mean diameter of the particles is in the exaction size regime (i.e. 10 nm) [61–69]

Various nanostructures have been investigated to determine their properties and possible applications in biosensors. These structures include nanotubes, nanofibers, nanorods, nanoparticles and thin films.

Nanoparticles have numerous possible applications in biosensors. For example, functional nanoparticles (electronic, optical and magnetic) bound to biological molecules (e.g. peptides, proteins, nucleic acids) have been developed for use in biosensors to detect and amplify various signals. Some of the nanoparticle-based sensors include the acoustic wave biosensors, optical biosensors, magnetic and electrochemical biosensors, as discussed next. [70]

Nanoelectrodes can be categorized as individual nanoelectrodes, nanoelectrode arrays (NEAs), or nanoelectrode ensembles (NEEs). [71, 72] Individual nanoelectrodes have been produced from carbon fibers and metals, such as platinum and gold wires, produced by flame- or electrochemical-etching methods [71, 72]. The active radii of electrode tips are from a few tens to several hundreds of nanometers, with varying surface roughness. Carbon fiber nanoelectrode can be produced with very smooth surfaces, as verified by scanning electron microscopy. Carbon nanotubes (CNTs) and metal nanowires can be assembled in densely packed arrays of NEAs and NEEs. The alignment of individual nanoelectrodes can vary from well-ordered periodic arrays to random collections of nanostructured materials. These platforms have been produced from CNTs, pure metallic nanowires, metal oxide nanowires, and magnetic nanoparticles [71, 72]. The geometric order of the platforms differentiates arrays from ensembles; NEAs consist of periodic arrangement of individual nanoelectrodes, whereas NEEs are more random collections of nanoelectrodes.

1.8 Self Assembled Monolayer Modified Electrodes

In the last years, chemical modified electrodes by self assembled monolayer of alkanothiols have been extensively used because their simplicity and efficiency [73]. The functionalization of such self-assembled monolayer is important issue today because molecular architecture can be build which confer new surface properties [74, 75]. The design and construction of such novel molecular devices is opening a huge number of applications in areas such as corrosion protection, wetting, microelectronics, optics, chemical, biochemical and electrochemical sensors [76-80]. Despite the great versatility and perspectives show by electrochemical sensors, the utility of an electrode is limited by gradual degradation of its surface. From this point of view, the gold surface is a preferred one, because has the third best electrical conductivity of all metals at room temperature and its inertness prevent the formation of insulating surface oxides [77, 79].

1.9 Gold electrodes in biosensor fabrication

Gold electrodes have been increasingly used in designing electrochemical biosensors because they allow durable immobilization of biomolecules to the electrode surface while controlling the molecular architecture of the recognition layer, most often via binding to self-assembled monolayers (SAMs) [80, 84]. The gold surface modification with organic thiols compounds opens numerous opportunities for the construction of modified electrodes by using a well known and efficient reaction. In generally, such modified electrodes are obtained in two ways [85-87]: (i) adsorption of thiols on gold surface, followed by the adsorption of specific receptor on thiols monolayer (embedment procedure), or (ii) adsorption of functionalized thiols on gold surface, where the functional groups of thiols have the receptor role (Figure 1.4). In both cases, the performances of the obtained modifications are significant dependent by the gold surface quality. If the gold surface is the smooth-faced one, its cover degree is higher, the obtained monolayer is well ordered, and the electrodes have great analytical performances.

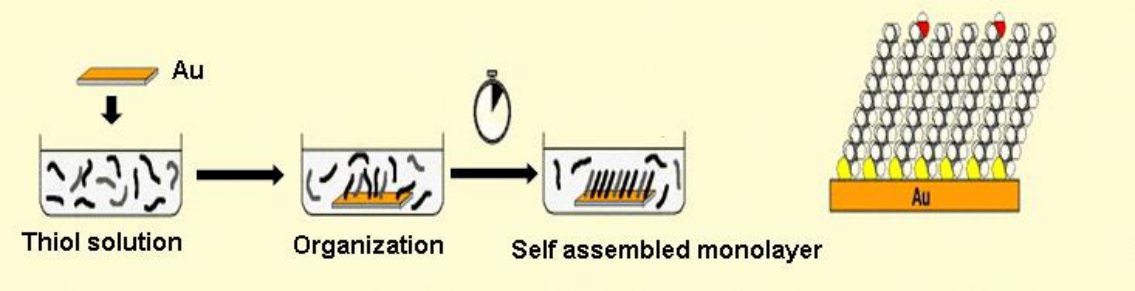

Figure 1.4 Formation of self assembled monolayer on gold

Enzyme immobilization on flat gold surfaces, however, often suffers from low amounts of biomolecules and poor electrical contact to the transducer. Actually, most efforts are directed to two new directions: (1) production of composite electrodes made of gold nanoclusters and immobilized enzymes, which exploit the enhanced catalytic activity of the gold nanoparticles [88-90], and (2) the three-dimensional structuration of gold electrodes with nanometer- sized dimensions for biosensor applications (e.g., microporous gold electrodes [91], nanopatterning of porous gold films [92] or gold nanoelectrode ensembles [93]).

1.9.1 Gold nanomaterials in enzyme biosensors

The electrodes are usually modified by gold nanomaterials in different ways to improve the performance of the biosensor. The electrode surface could be roughened by gold nanoparticles to enhance the interaction of enzyme or biomolecules with the electrode.

1.9.1.1 Gold nanoparticles

Gold nanoparticles could provide a stable immobilization for biomolecules retaining their bioactivity. Moreover, electron transfer between redox proteins and electron surfaces is facilitated, which is induced by many factors, such as the high surface-to-volume ratio, high surface energy, decreased proteins-metal particles distance and the functioning as electronconducting pathways between prosthetic groups and the electrode surface from the gold nanoparticles. Gold nanoparticles are normally synthesized by chemical route and electrodeposition. Pingarron et al. recently reported a review on gold nanoparticle-based electrochemical biosensors, in which gold-based enzyme biosensor are summarized [94]. An example is the construction of acetylcholinesterase biosensor in

which electrode was modified by electrodeposited gold nanoparticles at the electrode surface after hydrolysis of acethlthiocholine by the immobilization enzyme [95]. This method is valuable for the development of new devices for the sensitive detection of potentially dangerous and deadly neurotoxins. Carbon paste electrode could be modified by the colloidal gold consisting of pretreated graphite power with colloid gold solution and paraffin oil [96]. GOD was immobilized onto the modified electrode via physical adsorption. Such kind of GOD biosensor can efficiently exclude the interference of commonly coexisted uric and ascorbic acid [97]. The similar methodology is also favored for other substrate detection, such as phenol and hydrogen peroxide [96-98]. Gold electrode can be modified by attachement of gold nanoparticles via covalent bond. These gold nanoparticles by chemical route were self-assembled on gold electrode by dithiol via Au-S bond, where dithiol was physically absorbed on the electrode surface by putting gold electrode immersed into a dithiol ethanol solution [99]. A cystamine monolayer was then chemisorbed onto those gold nanoparticles and exposed to an array of amino groups, after that GOD was immobilized by covalently attached to the cystamine modified electrode [99]. Zhang et al., reported that the biosensor provided a linear response to glucose from 20 µM – 5, 7 mM with a sensitivity of 88 µA/cm^2 mM. The sensor had a good reproducibility and remained stable over 30 days [99].

1.9.1.2 Gold nanocomposites

A wide variety of matrices, including inorganic materials, organic polymers, and other commercially available solid supports, have been used for enzyme immobilization. Chitosan, as mentioned in pervious part, is one of the most promising immobilization matrices due to its excellent properties. Colloidal gold nanoparticles have been also used as the matrix for the enzyme immobilization to retain the macromolecules' bioactivity. The adsorption of colloidal gold nanoparticles on the chitosan membrane could provide an assembly of gold nanoparticle mulilayers and a suitable microenvironment similar to the native environment of biomolecules. Based on this approach, a disposal biosensor was fabricated for the rapid detection of H_2O_2 by entrapping HRP in colloidal gold nanoparticle modified chitosan membrane [96, 97]. The biosensor was characterized with good detection precision and storage stability. Based on a similar methodology, glucose [100] and HRP [101] biosensors were prepared by self-assembling gold nanoparticles on chitosan hydrogel modified Au electrodes. Nanocomposites by combination of gold nanoparticles with inorganic or organic nanomaterials have shown to possess interesting properties, which can be profited for the development of electrochemical biosensors. An

example of such nanocomposites is a colloidal gold-CNT composite electrode using Teflon as the non-conducting binding material [102]. The constructed biosensor showed significantly improved responses to H_2O_2, and the incorporation of GOD into the new composite matrix allowed the preparation of a mediator less glucose biosensor with a remarkably higher sensitivity than that from other GOD-CNT bioelectrodes [102]. Hybrid nanocomposites of gold nanoparticles and organic materials are proposed, in which gold and polypirrole (PPy) are fabricated by wet chemical route using chloroauric acid ($HAuCl_4$) and pyrrole as the reaction reagents [103]. The reaction occurs in mild aqueous conditions and doesn't involve application of an electrical potential, surfactants or solvents that could affect the biological activity. A stable nanocomposite strongly adhered to the surface of glassy electrode carbon (GCE) electrode and could be employed for electrochemical characterization without loss of the immobilized material.

1.9.1.3 Gold nanoarrays

Many different metals have been electrodeposited using anodic alumina and nuclear track-etched polycarbonate. Electrodeposition inside nanoporous membrane templates [104, 105] has proved to be a versatile approach to fabrication of freestanding metallic nanowires. In general, nanoporous templates are widely available and relatively inexpensive: templates permit the preparation of materials with a high degree of homogeneity and reproducibility. Gold nanoarrays are a widely used nanoelectrode platform, which can be facilely prepared through the templated synthesis methods and other approaches. [71, 72] An apparent advantage of gold nanoelectrode ensembles (GNEEs) is an enhanced signal-to-background current ratio, leading to enhanced detection limits. [71, 72] Recently, three dimensional (3D) structured NEEs have aroused considerable interest for electrochemical studies and application because of their unique configurations and large surface areas. [71, 72] The 3D structured NEEs are typically produced by etching upper layers of the template membrane from a flat two-dimensional (2D) array, creating additional surfaces and chemistries for detection. The ability to devise catalytic properties in gold NEEs make these very attractive for fabrication of electrochemical sensors for use in clinical diagnostic applications. These results indicate that GNEE is a good immobilization matrix, providing a large well-defined surface area with the capacity to modify the nanowire surfaces by linking to proteins. The prospect of spatial patterning with biomolecules is limited by maintaining the active and functional state of the protein. Approaches to orient and retain the electroactive states of these biomolecules can lead to enhanced sensitivities. The use of spacers has led to increased

activities by decreasing deleterious surface effects, such as denaturation and unfolding of proteins onto electrodes or assemblies. [106, 107, 108].

1.10 Flow Injection Analyses

Flow injection analysis (FIA) is one of the most powerful analytical tools to monitor automatically a large variety of *on-line* processes for multi-components systems. The application of this methodology in biosensing systems has been showed very useful to investigate the main sensor parameters. Theoretical considerations about the dependence of the signal upon the experimental parameters, i.e. the diffusion flow rate and the geometric configuration, have been also performed compared to continuous flow techniques.

1.10.1 Basic Components:

The basic scheme of an FIA system is showed in Fig. 1.5 and consists of four essential components:

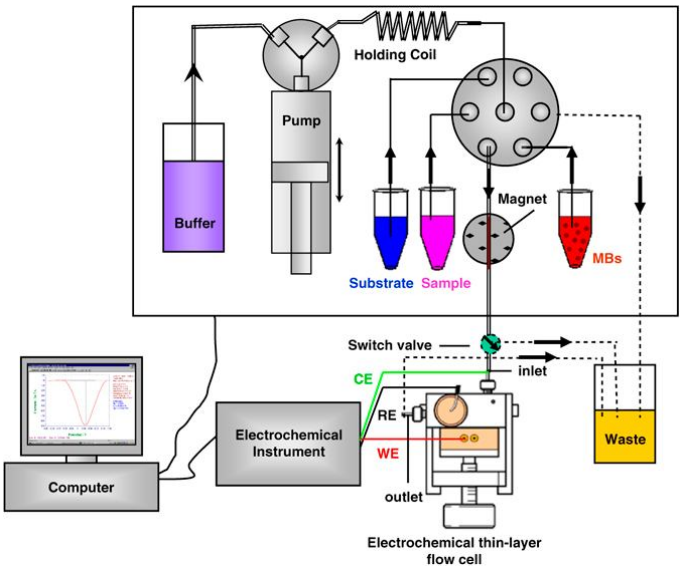

Figure 1.5 Flow Injection Analysis System

a) A ***propelling unit*** which produces the flow of one or more solutions, either containing reagents or merely acting as the carrier(s).The propelling system must force the carrier stream through the units, in a perfectly reproducible, pulse-free and as constant as possible flow rate. This function can be performed by a peristaltic pump (the most used in FIA applications, up to now), a gas-pressure system or even gravity-based units;

b) An ***injection system*** which allows the reproducible insertion or introduction of an accurately measured reproducible sample volume into the flow, without stopping it [109];
c) A **length of tubing**, commonly, and sometimes improperly, called the ***reactor***, along with the transport operation takes place, with or without an additional process. The role of the reactor can be played by a straight, coiled or knotted tube (which may also be packed with inert beads), or by a mixing chamber or a tube packed with a chemically active material, such as redox, ion-exchange resin, immobilised enzyme, etc.;
d) A ***flow cell***, accommodated in a detector (which can be a colorimeter, photometer, fluorimeter, potentiometer and mostly amperometer) which transduces some analytic property into a continuous signal to a recorder and/or microcomputer.
The flow emerging from the sensing system usually goes to waste, although it sometimes recirculates through the peristaltic pump to achieve constancy in the flow rate, or to allow use of recently developed additional techniques. The automatization of FIA requires the incorporation of a sampling system, a sample withdrawing system (generally involving the use of the peristaltic pump itself) and an electrically controlled injection system working in a co-ordination with the sampler. A micro-computing system with active interface allows the easy programming of this operation.

1.10.2 Methodology of Flow Injection Analysis

Flow injection analysis is a methodological innovation of the popular analytical tool, characterised by its versatility, reproducibility, simplicity, inexpensive, low sample consumption, low reagent consumption, short analysis time and it accommodates separation techniques. The term FIA was coined by Rûzicka and Hansen in 1975, studying the first injection system which made use of a hypodermic syringe to inject the sample into a reagent stream [110]. It is based on the injection of a liquid sample into a moving, nonsegmeted continuous carrier stream of a suitable liquid. The injection sample forms a zone, which is then transported toward a detector that continuously records the absorbance, electrode potential or other physical parameter as it continuously change due to the passage of sample material through the flow cell (Fig. 1.6).

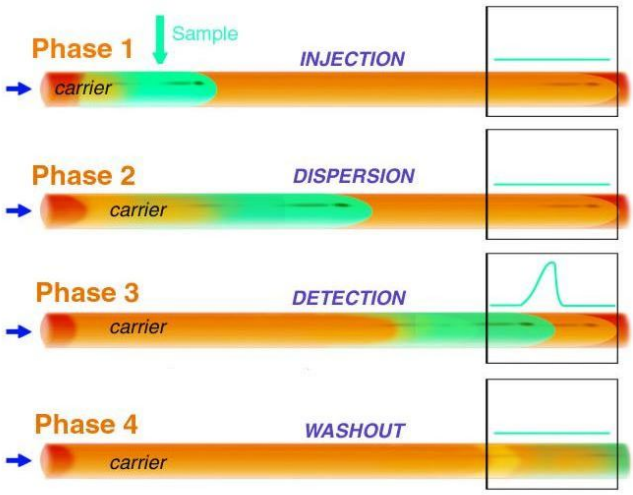

Figure 1.6 Four phases of Flow Injection Analysis

Due to their properties it is possible to use small volume of sample with less reagent consumption. Physical foundation of FIA is related to the concept of ***dispersion***, i.e. the dilution of a volume of sample into a carrier non-segmented stream. In order to quantify this phenomenon, Ruzicka and Hansen described a serie of experiments that would measures this expansion. They called this process dispersion.
Dispersion was then defined as the amount that the signal is reduced by injecting a sample plug into FIA- system. This is represented mathematically by:

$$D=C^0/C^{max}$$

where D is, the dispersion coefficient at the peak maximum produced by the ratio between C^0, the concentration of a pure dye, and C^{max}, the concentration of that same injected dye as it passes through the detector.
Dispersion can be classified as limit (D= 1-3), medium (D=3-10) and large (D>10)

1.10.3 The importance of Dispersion

The dispersion coefficient is useful in that it allows comparisons of different manifolds. Further, is provides a means of verifying and monitoring the extent of sample dilution resulting from any changes made to the manifold during method development. In essence, what Ruzicka and Hansen called controlled dispersion is in fact the recognition

that the sample is reproducibly diluted as it travels down tubing. The reproducible timing allows for reproducible physical mixing and dilution. The dispersion is controlled.
However, the amount and direction of dispersion is not uniforthe entire sample zone. The centre of the zone is moving faster than edges against the wall, as wall drags slows the molecules. This is called axial dispersion (or convective dispersion). The molecules against the wall also move back toward the centre of the tubing. This is radial dispersion (causes by diffusion of molecules) of the system. Both radial and axial dispersion occur as the zone moves down the tubing.

1.10.4 Factors affecting controllable sample dispersion

In practice, the analyst controls the amount of sample dispersion by altering the manifold design. This controllable sample dispersion allows for a large degree of flexibility for the analyst. Factors that influence dispersion are:

- The volume of the sample, the larger volume, the smaller the dispersion. Note that at large sample volumes, the dispersion coefficient becomes unity. Under these circumstances, no appreciable mixing of sample and carrier takes place, and thus no sample dilution has occurred. Most flow injection analyses, however, involve interaction of the sample with the carrier or an injected reagent. Here, dispersion greater than unity is necessary. For example, a dispersion of two would be required if the sample and carrier are to be mixed in a 1:1 ratio;
- The length of the reactor tube: the larger this length, the greater the dispersion;
- The tube diameter: the dispersion is directly proportional to the diameter;
- The flow velocity (pump rate)

Furthermore, the form of the tube to the detector can also influence the dispersion. This tube can be straight, coiled or knitted. The knitted tubes give more dispersion then the coiled one and the coiled tube gives more dispersion than the straight tube.

1.10.5 The concentration gradient

Earlier, the dispersion coefficient at the peak maximum was discussed and defined as

$$D=C^0/C^{max}$$

However, essentially every section of the peak can be represented by a dispersion coefficient as defined by:

$$D=C^0/C$$

where C^0 is the concentration of the dye solution used injection and C is the measured concentration of the injected, disperse dye, $0<C<C^{max}$. This suggests a unique feature of the FIA peak, that is, for every rising portion of the peak, there is an identical point in terms of ration between R (reagent), S (sample) and RS on the falling portion of the peak. The dispersion coefficient is then the same for both points. These points are as reproducible as the peak maximum. That a reproducible concentration gradient exists is a unique characteristic of FIA [111].

1.10.6 Flow Injection Analysis Signals

As with the foremost analytical techniques, the response of the FIA detection unit is a transient signal which result from two consecutive processes, one of which time-dependent. FIA measurements are made when equilibrium condition has not been reached. This is a plot of analytical signal (absorbance, fluorescence, potential, etc.) as a function of time, expressed in seconds or minutes (fast or normal recordings). A typical recorder output has the form of a peak, Fig. 1.7, the height h, width W, or area A of which is related to the concentration of the analyte. In order to define a FIA recording, at least semi quantitatively, it is necessary to know its essential features:

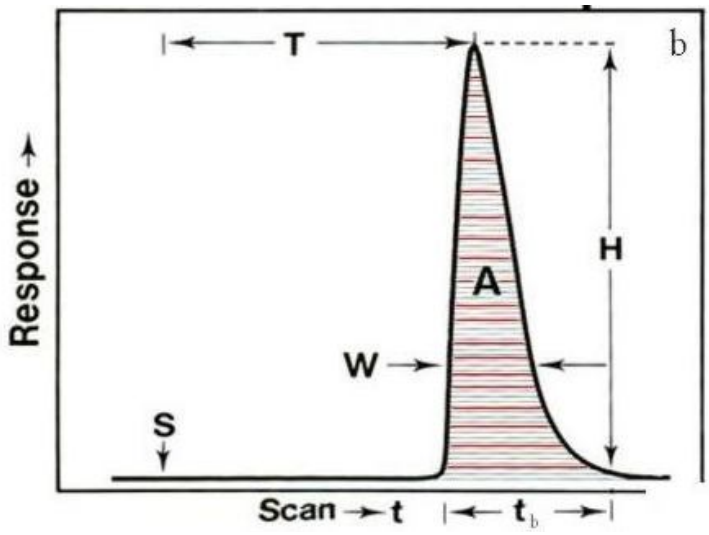

Figure 1.7 The analog output has the form of a peak, the recording starting at S (time of injection to). h is the peak height, W is the peak width at a selected level, and A is the peak area. T is the residence time corresponding to the peak height measurement, and tb is the peak width at the baseline.

The time span between the sample injection S and the peak maximum, which yields the analytical readout as peak height h, is the residence time T during which the chemical reaction takes place. A well-designed FIA system has an extremely rapid response, because T is in the range 5 - 20 s. Therefore, a sample cycle is less than 30 s (roughly T + tb) and thus, typically, two samples can be analyzed per minute. The baseline (tb) is an actual measure of the dispersion or dilution of the analyte, for it represents the time taken by the sample to pass through the detector. The injected sample volumes may be between 1 and 200 µL (typically 25 - 50 µL) which in turn requires no more than 0, 5 mL of reagent per sampling cycle. This makes FIA a simple, automated microchemical technique, capable of a high sampling rate and minimum sample and reagent consumption. FIA is a general solution-handling technique, applicable to a variety of tasks ranging from pH or conductivity measurement to colorimetry, titrations, and enzymatic assays. To design any FIA system properly, one must consider the desired function to be performed.

1.11 Enzyme: Tyrosinase

Tyrosinases (EC 1.14.18.1 and EC 1.10.3.1) (Fig. 1.8), also termed polyphenoloxidases (PPOs), have been characterized from sources as diverse as bacteria, fungi, plants and animals and are usually associated with the biosynthesis of brown melanin pigments [112-115]. Tyrosinase is a copper-containing monooxygenase enzyme which catalyzes the conversion of phenolic substrates to catechol. Tyrosinases catalyse two reactions: (1) the hydroxylation of mono- to di-phenols, called the cresolase or monophenolase reaction, and (2) the oxidation of diphenols to o-quinones, which is referred to as the catecholase or diphenolase reaction. When tyrosine is used as a substrate, it is first hydroxylated to form 3-(3,4-dihydroxyphenyl) alanine (L-dopa) and then oxidized to dopaquinone, an unstable compound which polymerizes spontaneously to give rise to melanin pigments (Fig. 1.9).

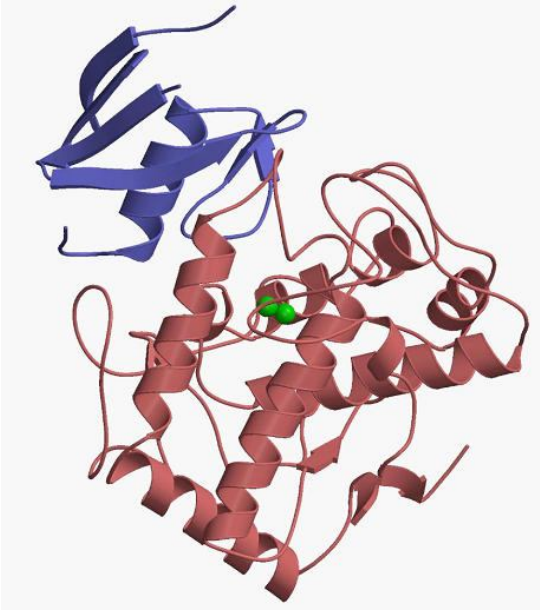

Figure 1.8 Tyrosinase enzyme 3D model

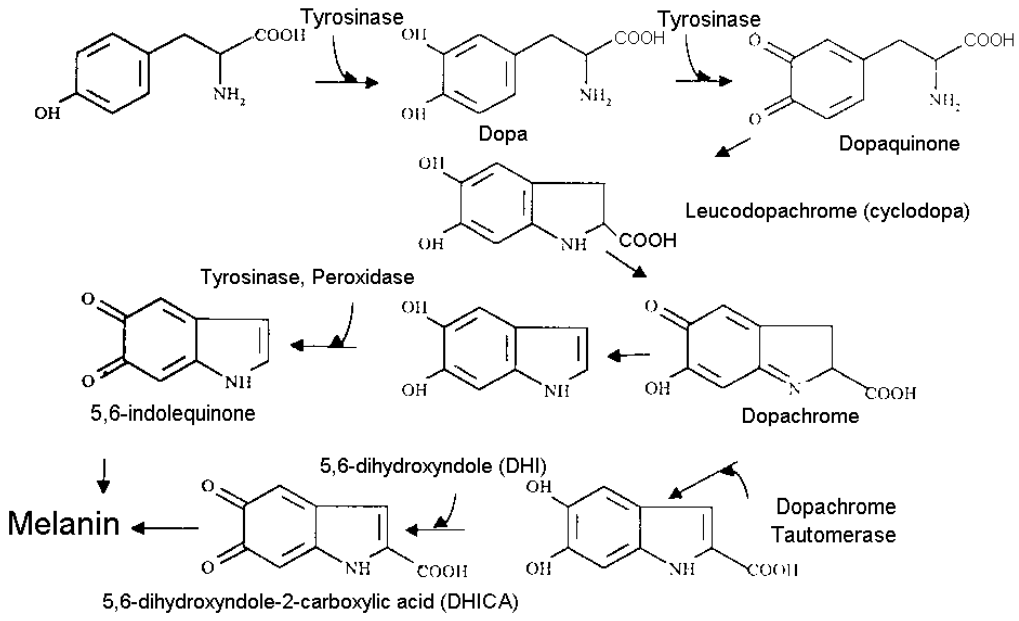

Figure 1.9 Intracellular transformation of tyrosinase into pre-melanin metabolites, and finally into melanin; several of the metabolites between tyrosinase and melanin are toxic to melanocytes according to the self-destruct theory.

The active site contains a binuclear copper cluster in tyrosinase from mushroom (Agaricus bisporus) and from human malignant melanoma [116, 117], hence the commercially available mushroom enzyme has been widely used as a model for mammalian tyrosinase. Most of the enzyme in a fresh preparation is in the met-tyrosinase form, in which the active site is bicupric and unable to bind oxygen. Only a relatively small proportion of the enzyme is present in the active monophenolase or oxy-form. This is produced when the met-form undergoes a two-electron reduction to the bicuprous state, which binds oxygen to form a bicupric-peroxide complex [118]. The initial rate of monohydric phenol oxidation is therefore slow unless a suitable two-electron reducing agent (e.g. L-dopa) [119] or a thiol compound [120]) is supplied exogenously. Generation of dihydric phenols from the o-quinone oxidation products (e.g. dopa from dopaquinone) provides an auto-activating mechanism, which results in a gradually accelerating rate of reaction.

1.11.1 Tyrosinase based electrochemical sensors

Electrochemical biosensors based on tyrosinase or polyphenol oxidases enzyme are considered as an alternative to the conventional techniques for phenolics determination due to their simplified sample treatment, portable, economical, fast and sensitive analysis [121, 122]. Several groups have investigated tyrosinase-based biosensors for the low potential detection of phenols and catechols in foods, pharmaceuticals, and clinical and environmental samples [123–128]. Tyrosinase-catalysed oxidation of tyrosine and of other monohydric phenols involves o-hydroxylation followed by oxidation of the dihydric phenol so formed to the corresponding o-quinone in a single step without release of the dihydric phenol intermediate. Usually, for amperometric detection of catechol, the subsequent electrochemical reduction of *o*-quinone is quantified by measuring the resulting reduction current. Quinones are electroactive species that can be reduced at low potentials [123]. Recent years, many amperometric biosensors based on the inhibition of the activity of tyrosinase enzymes have been used for the determination of triazine and phenylurea herbicides in the environment [129-132]. A key factor in the construction of a biosensor is the need to achieve adequate and effective enzyme immobilization. Some of the common approaches that have been used for the immobilization of tyrosinase on to various substrates include carbon paste immobilization [133, 134, 135], sol–gel immobilization [136-138], physical adsorption [139] and electrochemical entrapment of enzyme within polymer or composite matrix [140]. However, some of these methods are relatively complex. The solvents are disadvantageous to the environment. Therefore,

searching for a simple and reliable method to immobilize tyrosinase is of considerable interest [141].

1.12 Reasons to develop new sensors

The instability of the quinonoid oxidation products of tyrosinase substrates renders spectrophotometric estimations of the reaction kinetics by measurement of product chromophore accumulation unreliable. This is especially relevant to studies involving investigation of adduct formation by quinone products, since the absorption spectrum of the adduct is frequently markedly different from that of the original product [120]. This problem may be avoided by use of an oximetric technique to measure directly the progress of the reaction by means of the oxygen consumption. However, tyrosinase-based electrochemical biosensors on some substrates suffer from low stability and significant inhibition of enzyme by reaction products; both these factors deteriorate electrode characteristics in phenolic compounds determination. One of the major causes of poor stability is desorption of enzyme from electrode materials. Therefore, the search for reliable methods or electrode substrates that would be a strong and efficient bonding of tyrosinase is still interesting. Recent reports shows nanotechnology promotes the developments of tyrosinase based electrochemical biosensors (Table 1.2).

Table 1.2 Role of nanomaterials in tyrosinase based electrochemical biosensors

Nanomaterials	Analytes	Techniques	Range Limited	LOD	Ref.
Gold nanoparticules, Multi- walled carbon nanotubes	Dopamine	Amperometry	$1,0x10^{-8}$ to $6,0x10^{-6}$	$3,0\times10^{-9}$	139
Biopolymers films	Dopamine	Amperometric, Cyclic voltammetry	$2,0x10^{-6}$ to $1,0x10^{-5}$	$9,0x10^{-7}$	140
Fe_3O_4- chitosan nanocomposite	Dopamine	Amperometric	$2,0x10^{-8}$ to $7,5x10^{-5}$	$6,0x10^{-9}$	141
Biopolymers films	L-dopa	Amperometric, Cyclic voltammetry	$5,0x10^{-6}$ to $3,0x10^{-5}$	$1,0x10^{-6}$	140
Carbon nanotubes	L-dopa	Amperometry	$5,0x10^{-7}$ to $1,0x10^{-5}$	-	142
Biopolymers films	L-dopa	Amperometric, Cyclic voltammetry	$1,5x10^{-5}$ to $5,5x10^{-5}$	$7,0x10^{-6}$	140
Chitosan composite film	DOPAC	Amperometry	$6,0x10^{-6}$ to $2,0x10^{-4}$	$3,0x10^{-6}$	143
Carbon nanotube modified polypyrrole biocomposite film	Catechol	Amperometry	$3,0x10^{-6}$- $5,0x10^{-5}$	$6,71x10^{-7}$	119
Sonogel - carbon	Catechol	Amperometry	$1,0x10^{-7}$ to $3,0\times10^{-5}$	3×10^{-8}	145
Tyrosinase- Biopolymers films	4- Methyl catechol	Amperometric, Cyclic voltammetry	$3,0x10^{-5}$ to $1,2x10^{-4}$	$1,7x10^{-5}$	140
Carbon nanotubes	Phenol	Amperometric	$5,0x10^{-8}$ to $1,0x10^{-6}$	$1,4x10^{-7}$	144
Sonogel - carbon	Phenol	Amperometric	5×10^{-7} to 3×10^{-5}	3×10^{-7}	145

2. Experiments

2.1 Experimental Part

Electrochemical techniques like cyclic voltammetry and chronoamperometry were employed in different parts of the present work. Electrochemical cell assembly, instrumentation and other aspects that are common for most of the experiments are reported here.

2.1.1 Instrumentation

Autolab PSTAT 12 Potentiostat /Galvanostat (EcoChemie, Netherlands) was employed for most of the electrochemical studies. The GPES version 4.9 (EcoChemie, the Netherlands) software is used to perform a variety of electroanalytical techniques [1].

2.2 Cell setup

2.2.1 Static

A cell stand with an undivided cell was used. The cell was made up of glass having the capacity of 25ml and the teflon made top had three separate holes for the insertion of electrodes viz. working electrode, counter electrode and reference electrode. The gold disk working electrode (2 mm diameter) used in the present study was supplied by Metrohm. AgIAgCl and platinum wire were used as reference and counter electrodes respectively. The cell top also had the purging and blanketing facilities for nitrogen gas with separate tubes to remove oxygen gas and to maintain an inert atmosphere above the sample solution. The purging and blanketing were controlled through GPES software.

2.2.2 Flow wall jet -FIA

Metrohm 656 flow cell was modified and utilized. In FIA experiments, working electrode is embedded along one wall of the channel whereas the reference electrode (Ag/AgCl) is opposite and platinum electrodes as counter electrode. The FIA system consists Gilson Minipuls-3 peristaltic pump used to propel solutions, a Rheodyne 5020 valve to inject the solutions and Autolab PSTAT 12 potentiostat/galvanostat. To link the various components of the FIA set up, teflon tubing (0.5 mm) and teflon end fittings were used.

2.3 Scanning electron micrographs (SEM)

SEM images were obtained using JEOL scanning electron microscope (Model FEI Quanta 400FEGESEM/EDAX PEGASUS X4M).

2.4 Membrane templates

Polycarbonate Track-etched membranes (PCTE) (Whatman, UK) with pore size 50 nm, pore density of ≈ 6000 pores/cm^2 and thickness 6-14 µm were used as template for gold deposition.

2.5 Reagents and solutions

The chemicals trifluoroacetic acid (Sigma- Aldrich), tin(II) chloride (Sigma- Aldrich), nitric acid (65%, Carlos Erba), silver nitrate (Carlo Erba), sulfuric acid (96 %, Panreac), ethanol (Panreac), dichloromethane (Fluka), sodium sulfite (Riedel de Haën), sodium bicarbonate (Sigma- Aldrich), formaldehyde (Sigma- Aldrich), methanol (Sigma- Aldrich), L-dopa (Sigma- Aldrich), dopamine (Sigma- Aldrich), catechol (Sigma- Aldrich), phenol (Merck), ascorbic acid (Merck), glucose (Sigma- Aldrich), urea (Sigma- Aldrich), cystamine (Sigma- Aldrich), glutaraldehyde (GA, 2%, Fluka), sodium phosphate monohydrate (Riedel-de-Haën) and dibasic sodium phosphate (Riedel-de-Haën) were used as received. The gold plating solution used was a standard plating solution containing sodium gold sulphite [$Na_3Au(SO_3)_2$], which was obtained from Germany. Medical grade serum was used for interferences studies.

For addition of volumes Gilson Medical Electronics (*pipetman®)* micropipettes of 100 µL, 200 µL, 1000 µL, 5000 µL and 10 mL were used. All the electrochemical measurements were investigated in 0.1M phosphate buffered saline (PBS), pH 6.5 and different analyte (catechol, L-dopa, dopamine and phenol) at room temperature (25^0C). All pH measurements were made with the analyte in buffer medium using pH meter (GLP 22, Grison). All the solutions were freshly prepared with high purity water (*18.0 MΩ)* from a Millipore water purification system.

2.6 Methods

2.6.1 Pretreatment of gold disk electrode

The gold disk electrode was pretreated as following procedure. Gold electrodes were manually polished using 0.3 µm and 0.05 µm alumina slurry for 5 minutes. Then the electrodes were sonicated for in Milli-Q water 30 seconds to remove adsorbed alumina. Electrochemical cleaning was carried out using cyclic voltammetry with potential range between –0.3 V and 1.5 V at scan rate 100 mV/s 20 cycles in 0.5 M H_2SO_4.

2.6.2 Preparation of gold nanoelectrodes

A gold plating solution was prepared by dissolving Na_2SO_3 (3.2014 g, 0.127 M), $NaHCO_3$ (0.42005 g, 0.025 M), and 10 mL of HCHO (0.625 M) in 180 mL of water. The pH of this solution was adjusted to 10 by adding 1.8 M H_2SO_4 dropwise. The volume was adjusted to 200 mL by adding water. Twenty milliliters of this solution was pipette and mixed with 0.2 mL of gold sulphite solution. The pH of the solution was again adjusted to 10 by the dropwise addition of 1.8 M H_2SO_4 (≈0.1 mL). The sample vial was kept at 5 °C in a refrigerator while the polycarbonate membrane was prepared for electroless deposition of gold.

A polycarbonate membrane with 50 nm pores, was immersed in a solution of $SnCl_2$ and trifluoroacetic acid for 45 min. This solution was prepared by dissolving $SnCl_2$ (0.2464 g, 0.026 M) and 0.3 mL of CF_3COOH (TFA) in a 50 mL standard measuring flask using a mixture of methanol and water (50:50). An ammonical $AgNO_3$ solution was prepared by titrating 50 mL of 0.029 M $AgNO_3$ with concentrated ammonium hydroxide solution. The solution turned brown when one or two drops of ammonia were added and became colorless upon further addition of ammonia (≈0.5 mL). The membrane was removed from the $SnCl_2$/TFA solution and washed with methanol for 10 min. The membrane was then activated by immersed in the ammoniacal $AgNO_3$ solution for 10 min. The membrane was again washed with methanol thoroughly to remove the excess $AgNO_3$. The membrane was hung into the gold plating solution vertically using a clip for 24 h. The deposited gold on both faces of the membrane was gently removed using Q-Tips wetted with ethanol. The membranes were then immersed in 25% HNO_3 for 12 h to remove the surface-bound chemicals from the gold plating solution. Finally, the membrane was heated at 150 °C, the glass transition temperature of polycarbonate, for 10 min. This produces a water light seal

between the Au nanoarrays and polycarbonate pore walls necessary to avoid creeping of the solution into the junction which leads to higher values of background currents [142].

2.6.3 Etching Procedure

Etching of the polycarbonate membrane (PCTE) was carried out by using a mixture of dichloromethane (DCM) and ethanol (EtOH). The PCTE was found to be highly soluble in chloro solvents such as tetrachloromethane, chloroform, and dichloromethane and insoluble in methanol, EtOH, and ethyl acetate. Since the solubility of PCTE membrane in dichloromethane can be regulated by mixing with ethanol, a solvent mixture of dichloromethane and ethanol was chosen as the most suitable etchant to produce GNEEs, ultimately producing Au nanoensembles.

2.6.4 Enzyme Immobilization

Gold nanoelectrodes are potentially interesting for application in bio-chemical sensing devices. Thiol monolayer, cystamine, was employed as base interfaces to link the enzyme to the electrode support. The enzyme electrode forming process started with the introduction of amine functionalities on the Au surface by the chemisorption of cystamine (0.02 M, 18 h) using absolute ethanol as a solvent. The resulting aminated Au surface was modified by dipping in a solution of a 2% glutaraldehyde (GA) for 2 h at room temperature. In the system modified with cystamine, glutaraldehyde was using as a linking agent to carry out a covalent binding with the amine-functional group in Au electrode. For that purpose, tyrosinase (EC 1.14.18.1 and EC 1.10.3.1) was covalently immobilized onto preformed self-assembled alkylthiols monolayers on gold. An aliquot (50 µL) of tyrosinase solution, was then pipetted onto the surface of the modified gold nanoelectrodes. The sensor was placed at 4 ˚C for 24h for the enzyme immobilization. This tyrosinase immobilized electrode was then rinsed with a pH 6.5 phosphate buffer to remove any non-immobilized enzyme and the biosensors were stored at 4 ˚C until use. (Fig.2.1)

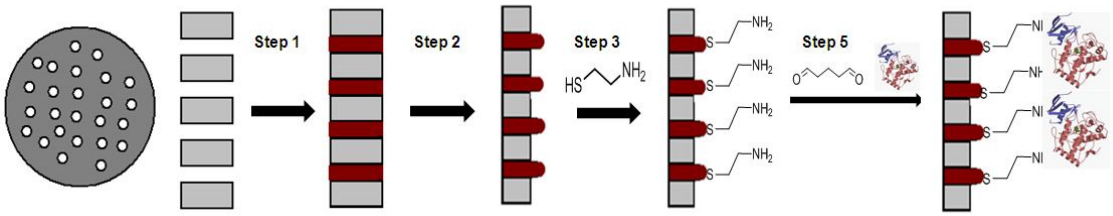

Scheme 2.1 Step 1- Electroless Au deposition, Step 2- Partial etching and exposing gold nanoarrays , Step 3- Aminoethnalthiol self assembled monolayer formation, Step 4 - Glutaraldehyde activation and Tyrosinase immobilisation

2.6.5 Interferences Studies

The electrochemical biosensor for catecholamines was held at -0.1 V, and 0.1 M ascorbic acid, 0.1 M glucose, 0.1 M urea and serum were injected in the electrochemical reaction cell consecutively. The response obtained was compared to the response of the other analytes (L-dopa, dopamine, catechol and phenol). To make sure ascorbic acid was not interfering with the measurements of other catecholamines, selectivity of the biosensor to the interferences was determined individually in the absence of any other interference.

2.6.6. Photographs of FIA step up

Figure 2.1 FIA set up

Figure 2.2 Autolab PSTAT 12 Potentiostat /Galvanostat

3. Results and Discussion

3.1 Results and discussion

Electroless metal deposition involves the use of a chemical reducing agent to plate a metal from solution onto a surface. The advantage of the electroless method (relative to electrochemical plating) is that the surface to be coated need not be electronically conductive. The key requirement of an electroless deposition bath of this type is to arrange the chemistry such that the kinetics of homogeneous electron transfer from the reducing agent to the metal ion is slow. This is essential because otherwise the metal ion would simply be reduced in the bulk solution. A catalyst that accelerates the rate of metal ion reduction is then applied to the surface to be coated. In this way, metal ion is reduced only at the surface, and the surface becomes coated with the desired metal (Scheme 3.1).

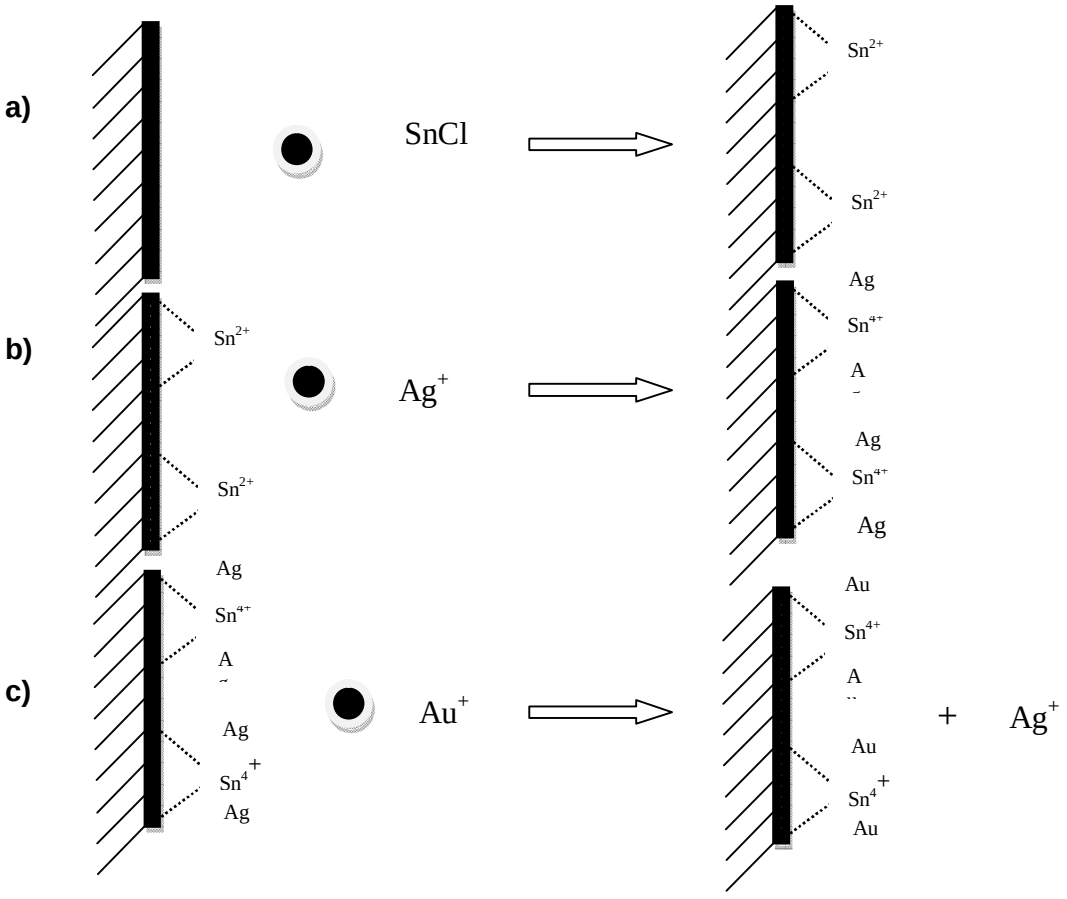

Scheme 3.1 Mechanism of electroless deposition of gold on the PCTE membrane pores

A "sensitizer" (Sn^{2+}) was first applied to the surfaces (pore walls plus faces) of the membrane. The Sn^{2+} adheres to the pore walls (Scheme 3.1a) and coated with a layer of gold during production. The Sn^{2+}-sensitized membrane was then activated by immersed in the ammoniacal $AgNO_3$ solution. This causes a redox reaction in which the surface bound, Sn(II) is oxidized to Sn(IV) and the Ag^+ is reduced to elemental *Ag;* some silver oxide is also obtained. As a result, the pore walls and membrane faces become coated with

discrete, nanoscopic *Ag* particles (Scheme 3.1b). The Ag particles are galvanically displaced by Au since gold is a more noble metal. As a result, the pore walls and faces become coated with Au particles (Scheme 3.1c). These particles are excellent catalytic sites for the oxidation of formaldehyde and the concurrent reduction of Au (I) to Au(0). As a result, gold plating continues on the gold particles, with formaldehyde as the reducing agent. The key feature of the electroless deposition process is that Au deposition begins at the pore wall. As a result, after brief deposition times, a hollow Au tubule is obtained within each pore.

The polycarbonate surface should be removable by a solvent in which the membrane dissolves. It is well known that polycarbonate dissolves in solvents such as chloroform and dichloromethane. Therefore, it is not possible to etch the polycarbonate using dichloromethane alone. Polycarbonate membranes are also insoluble in solvents such as ethanol, methanol, acetonitrile, and ethyl acetate. Thus, by mixing a dissolving with a nondissolving solvent, we found that it was possible to selectively etch the surface layers of Au filled polycarbonate membranes. For example, a mixture of DCM and EtOH in a solvent ratio of 50:50 resulted in controlled etching of the surface layers of Au-filled polycarbonate membranes. Preparation of gold nanowires in polycarbonate membranes and details of the chemical etching method are described in the Experimental Section. Briefly, the surface of the polycarbonate membrane was wiped with a Q-Tip dipped in the solvent mixture. After this solvent wipe, the solvent was allowed to dry and followed by another solvent wipe; the same procedure was repeated 10 times. The SEM of this membrane revealed Au nanowires protruding from the polycarbonate membrane. However, the slow evaporation of solvent after each solvent wipe left undesired voids on the polycarbonate surface. Such voids could be eliminated by wiping the polycarbonate membrane with a dry Q-Tip immediately after exposure to the solvent mixture. Thus, the surface of the Au-filled polycarbonate membrane was solvent wiped with a Q-Tip dipped in 50:50 DCM/EtOH mixtures, followed immediately by a dry wipe of the surface with a dry Q-Tip.

Scanning electron microscopy can be used to image the surface of the membrane after removal of the Au surface layer. An image of this type for a membrane that contained 50-nm-diameter pores is shown in Figure 3.1. The SEM observations, as the one reported in figure, show highly regular and uniform Au nanowires with an average diameter of 50 nm and a length of 180±20 nm. The image was obtained after etching away the Au layer grown over the front side of the template membrane. The SEM picture (Fig.3.1) of this

membrane shows the absence of voids on the surface, indicating that this method efficiently produces 3D GNEEs with protruding Au wires. From the figure, nanowires density can be also calculated of around 10 nanowires /μm^2, in accordance with the declared pore density, thus confirming each template pore was filled with gold. The etching rate was reproducibly controlled by restricting the quantity of solvent mixture applied to the membrane surface, as described before. Accordingly, good electronic conduction was established between the nanoelectrode ensembles and the copper tape when GNEEs was connected to the external circuit. Since electrons are capable of penetrating through some finite thickness of the polycarbonate membrane, small portions of the Au nanowires in the angled tracks are visible.

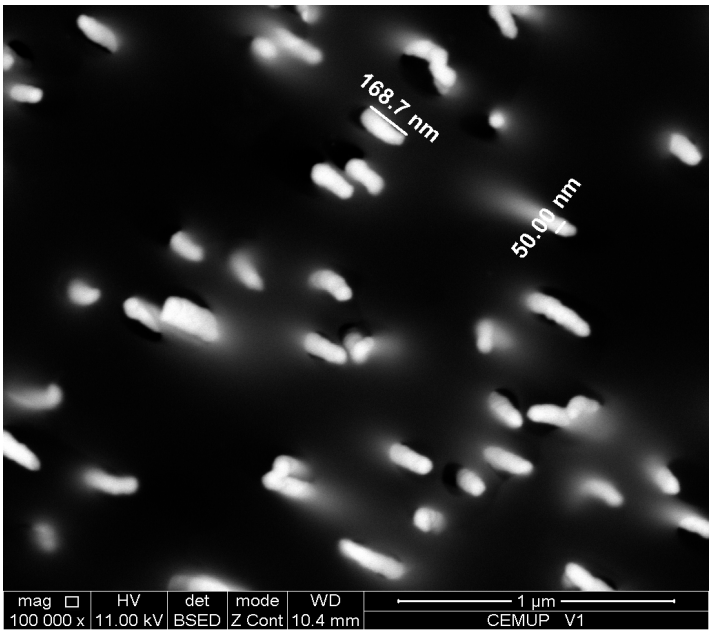

Figure 3.1 SEM image of 3D GNEEs created using a 50:50 DCM/EtOH mixture applied to a Au-filled polycarbonate membrane (50 nm- diameter pores).

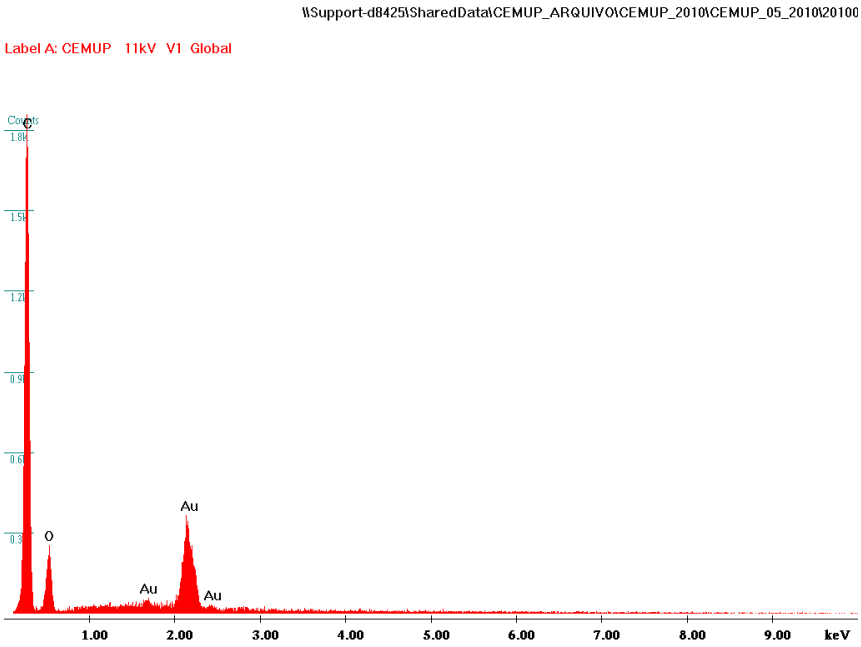

Figure 3.2 EDX spectrum of Au filled PCTE membrane before etching (2D).

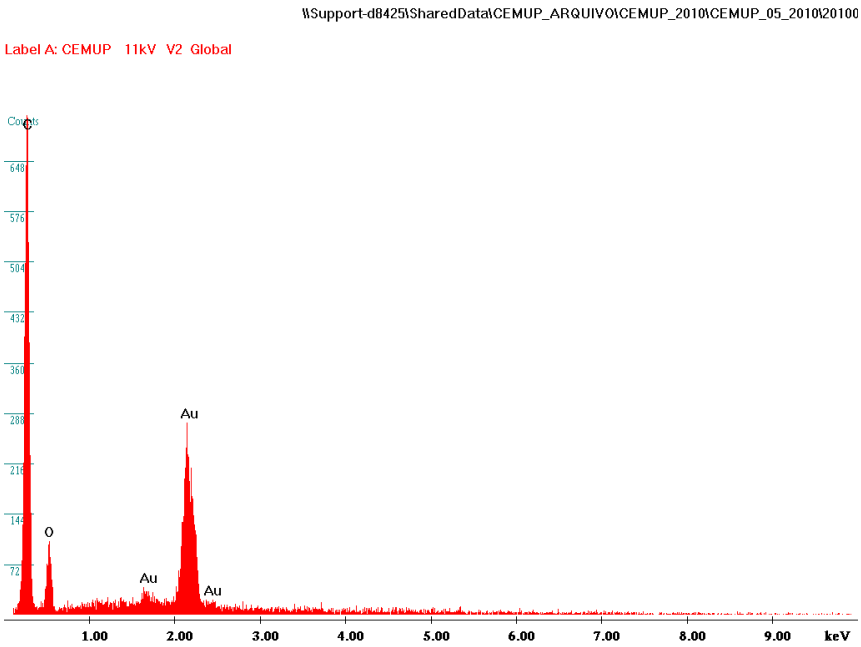

Figure 3.3 EDX spectrum of Au filled PCTE membrane before etching (3D)

The results of energy dispersive X-ray (EDX) technique in Fig. 3.2 show the nanowires were pure Au even though there were sensitization, activation and displacement reactions in the deposition steps, in which tin and silver were included in the catalysis reaction on

the surface of the membrane. The larger Au EDX peak intensity of the etched membrane relative to a representative unetched membrane (Fig. 3.3) demonstrates that the area of each Au-filled pore in the membrane has increased in the case of the 3D GNEE. These studies also evidenced that this procedure minimized chemical contamination from the process of gold deposition during the preparation of GNEEs.

3.2 Electrochemical characterization of GNEE

A persistent problem with nanoelectrodes is the sealing of the conductive element to the insulating material that surrounds the element such that solution does not creep into this junction. This solution creeping is undesirable because it causes the double-layer charging currents to be spuriously large [143,144]. The polycarbonate membranes are stretch-oriented during fabrication in order to improve their mechanical properties. If the membrane is subsequently heated above its glass transition temperature (150 *ºC),* the polymer chains relax to their unstretched conformation and the membrane shrinks. This shrinking of the membrane around the Au nanowires in the pores causes the junction between the nanowire and the pore wall to be sealed.

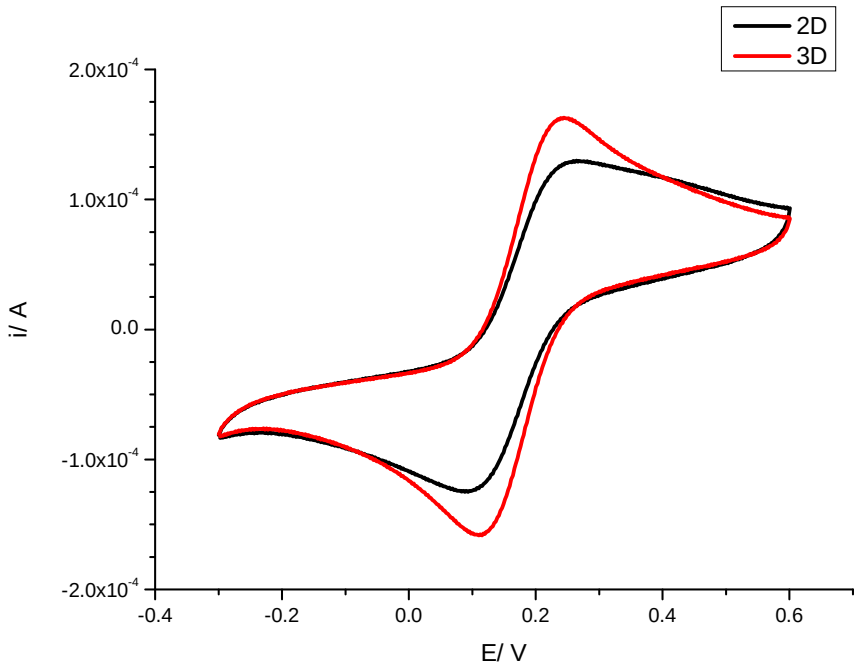

Figure 3.4 Cyclic voltammograms obtained at 3D and 2D GNEEs in 0.001M $K_3[Fe(CN)_6]$ in 0.1 M KNO_3 at a scan rate of 50 mV/s.

The Fig. 3.4 presents cyclic voltammograms 1: 1 0.01 M $K_4[Fe(CN)_6]$ and $K_3[Fe(CN)_6]$ 0.1 M KNO_3 of unetched (2D) and etched (3D) side of membrane, with a potential of working electrode between -0.3 V and 0.6 V obtained using GNEE. The very low double layer charging current indicates the satisfactory sealing treatment between the conducting Au nanowires and polycarbonate membrane. A peak-shaped CV results due to the close spacing of the 10 nanowires/μm^2 Au-filled pores in the exposed geometric area so that the overlap of individual diffusion layers results in the creation of an apparent planar diffusion layer that extends over the entire GNEE. Thus, the GNEE behaves like a large electrode with a surface area equal to the total surface area of the ensemble, including the active and nonactive surface areas.

The larger peak current and the smaller peak separation of the 3D cylindrical GNEEs than those of unetched 2D disc GNEEs demonstrate that the 3D cylindrical GNEEs can greatly increase the ratio of signal to background current. The smaller peak separation values at the 3D cylindrical GNEEs could be ascribed to the faster electron transfer process than that at the 2D disc GNEEs.

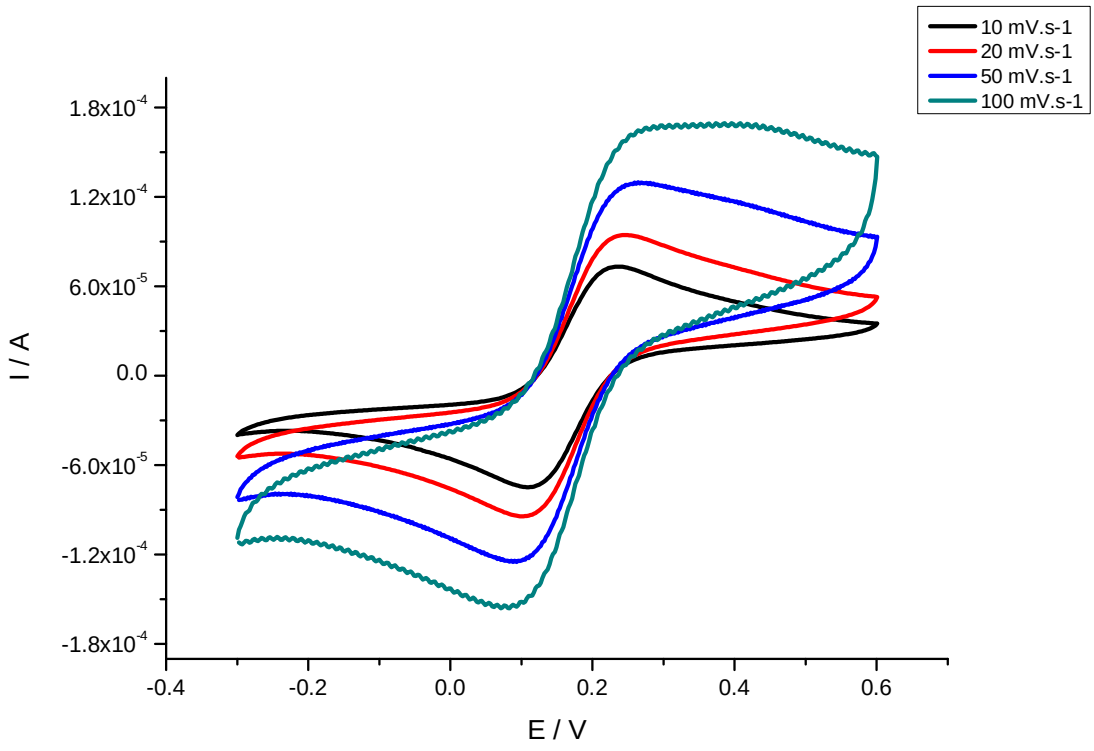

Figure 3.5 Cyclic voltammograms obtained at different scan rates for 2D GNEEs in 0.01M $K_3[Fe(CN)_6]$ and PBS, pH 6.5 at scan rates ranging from 10 to 100 mV/s.

Figure 3.5 and Fig. 3.6 shows voltammogramms at various scan rates for ferricyanide [Fe (CN) $_6$]$^{3-}$ with 2D and 3D GNEEs. The peak separation (ΔE_{pk}) values are shown in Table 3.1. This couple shows reversible voltammetry ($\Delta E_{pk} \approx$ 59 mV) at the lowest scan rates shown, for 2D and 3D GNEEs, but the voltammograms of 2D become quasireversible at scan rates above 0.01V. s^{-1}. (Table 3.1)

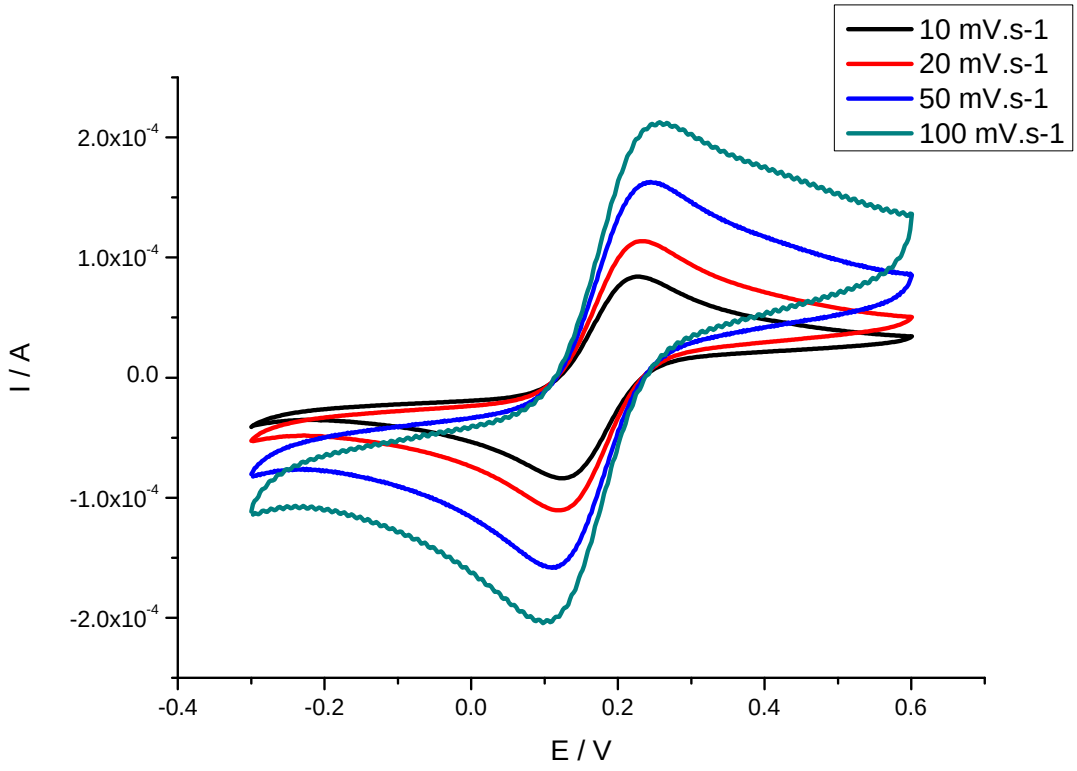

Figure 3.6 Cyclic voltammograms obtained at different scan rates for 3D GNEEs in 0.01M $K_3[Fe(CN)_6]$ and PBS with pH 6.5 at scan rates ranging from 10 to 100 mV/s.

Table 3.1 ΔE_{pk} values as a function of scan rates for 2D and 3D GNEEs.

	ΔEpk (mV)	
Scan Rate mV/s	**2D**	**3D**
10	67	63
20	72	65
50	92	68
100	102	75

The 2D GNEES shows reversible voltammetry at 10 and 20 mV/s scan rates. The transition from reversible to quasireversible appeared at lower scan rates than what would be observed at the 3D GNEEs that had reversible voltammetry for all scan rates. This is

because the 2D GNEEs was not exposed to a etching procedures and behaved like partially blocked electrode surfaces and the electron transfer processes seems less reversible than those at a 3D GNEEs. The effect of quasireversible electrochemistry is also clearly seen in the diminution of the voltammetric peak currents at 2D GNEEs relative to 3D GNEEs. The above voltammetric data for 3D GNEEs were also subjected to semiquantitative analysis by plotting log I_{pc} versus log v, where I_{pc} is the catodic peak current in the voltammogram and v the scan rate as show in Fig. 3.7.

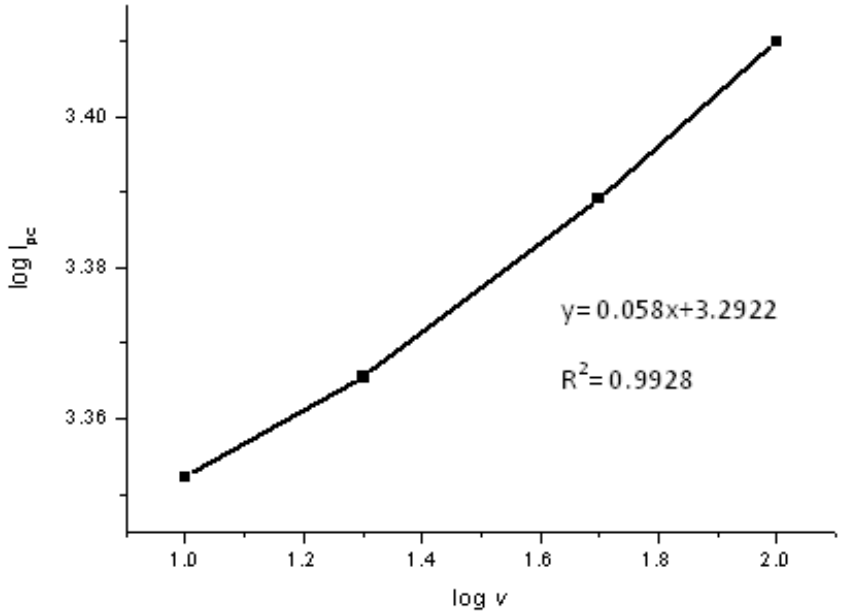

Figure 3.7 log I_{pc} vs. log v for cyclic voltammogram of 0.01M $K_3[Fe(CN)_6]$ and 0.1M PBS with pH 6.5 obtained used 3D GNEEs.

The slope is about 0.05 which demonstrate that a linear diffusion is dominant on the 3D GNEEs at conventional scan rates. The current that flows through an amperometric sensor introduced in a solution containing an inert background electrolyte (that provides the necessary electrical conductivity), and an electroactive species have two components: the non-faradaic current and the faradaic current. A nonfaradaic process involves the accumulation of charges at the electrode/solution interface; the structure formed in this process is called the electrical double layer: The double layer works as a capacitor. The double layer capacitance depends on the solution composition and also depends on potential applied to the electrode, and it is a measure of the ability of the electrical double layer to store electrical charge as a capacitor. Non-faradaic processes occurring at

electrodes cause a flow of non-faradaic currents (also called charging currents or capacitive currents), and account for the charging rate of the electrical double-layer at an electrode– solution interface. This current does not involve any chemical reactions (charge transfer), it only causes accumulation (or removal) of electrical charges on the electrode and in the electrolyte solution near the electrode. Non-faradaic currents are usually non-specific and they are rarely used to provide analytical signals; however, these currents contribute to the background noise and limit the detectability of controlled-potential techniques. Faradaic currents correspond to the electroreduction or electrooxidation of electroactive substances and, accordingly, are associated with electron transfer across the interface; species present in bulk solution may be reduced or oxidized only if they are brought to the electrode surface via a mass transport process (diffusion, migration and convection). In particular, the term diffusion describes faradaic current whose magnitude is controlled by the rate at which an electroactive species diffuses toward an electrode–solution interface. The nature of the faradaic currents observed at a GNEE depends on the distance between the electrode elements and the time scale (i.e., scan rate) of the experiments. The GNEEs used here are in the “total-overlap” response regime. In this total overlap regime, the diffusion layers at the individual elements of the GNEEs have overlapped to produce a diffusion layer that is linear to the entire geometric area of the GNEEs.

3.3 Self-assembled monolayers on GNEE

The adsorption of thiols on gold surfaces has recently attracted considerable interest, as it has been shown that such adsorption can result in the formation of well-organized self-assembled monolayers. Cystamine have frequently been employed as bifunctional building blocks, where the sulfur atoms of the molecules bind to the gold surface while the amino groups may be employed for the attachment of other groups to the self-assembled thiol layer. The electrochemistry of cystamine monolayer on GNEE was studied in a 0.01M 1:1 $K_3[Fe(CN)_6]$ and $K_4[Fe(CN)_6]$ in 0.1M PBS 6.5 by recording cyclic voltammograms in the potential region between -300 and 600 mV, using a SAM-GNEEs. The redox peak currents at SAM-GNEEs are larger than bare GNEE. The reversible redox reaction at the SAM-GNEE surface was facilitated by the positively charged protonated amino head group of self assembled monolayer on GNEE. The present experimental result supports that formation of cystamine SAM on GNEE (Fig. 3.8).

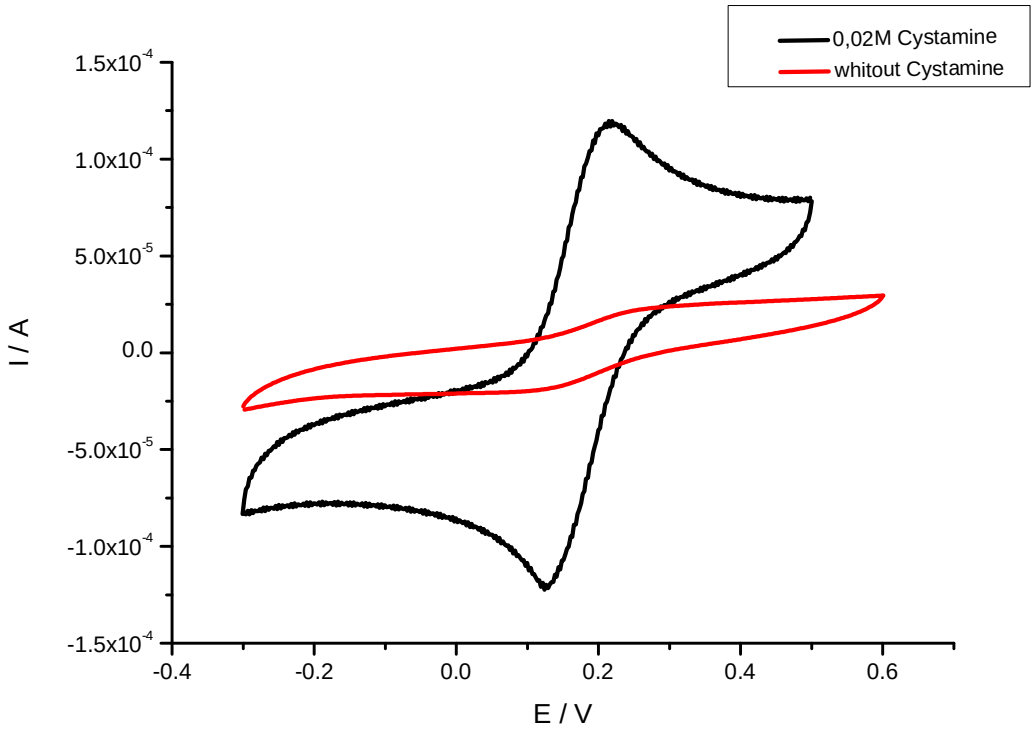

Figure 3.8 Cyclic voltammograms for SAM modified GNEEs and bare GNEE in a 0.01M 1:1 $K_3[Fe(CN)_6]$ and $K_4[Fe(CN)_6]$ in 0.1M PBS, pH 6.5.Scan rate 100 mV/s.

3.4 Electrochemical studies of Tyrosinase immobilized on GNEE

In the system modified with NH_2 terminated thiol, the TyrE molecules were covalently attached by glutaraldehyde as a linking agent. The effectiveness of this method in the enzyme immobilization procedure on the Au surface has been reported elsewhere [142]. The difference of cyclic voltammograms between the unmodifed GNEE and the tyrosinase electrode illustrates that tyrosinase has been immobilized successfully on GNEE through cyctamine self assembled monolayer (Fig. 3.9). Cyclic voltammograms of enzyme electrode recorded in PBS (0.1 M, pH 6.5) are shown in Fig. 3.9. A reversible redox peak for the enzyme electrode centered at $E_{1/2}$ 0.143V, corresponding to Cu^{2+}/Cu^{1+} redox center of TyE molecules, was observed.

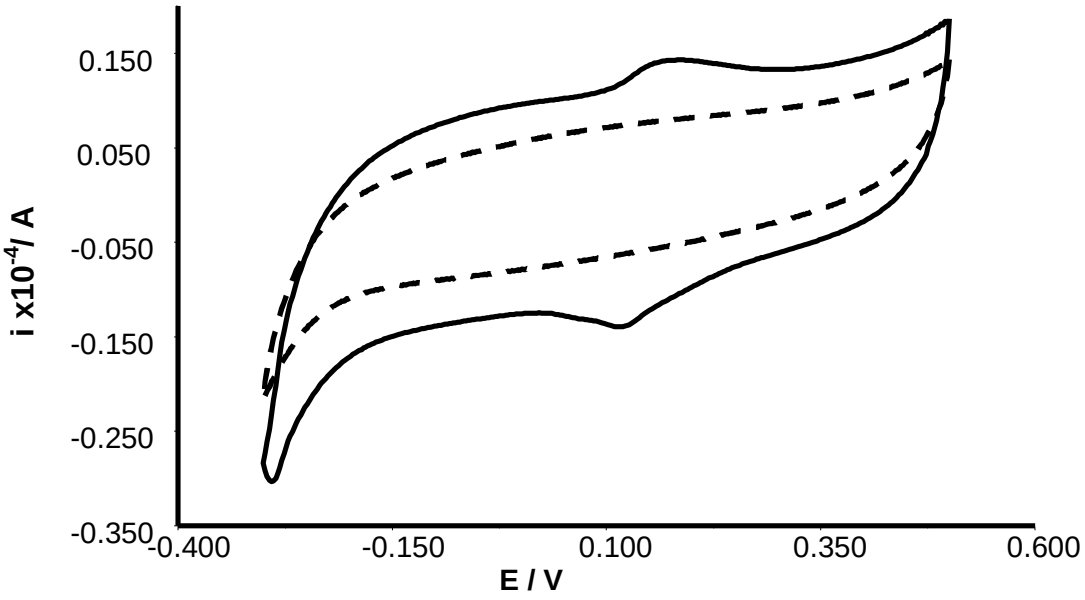

Figure 3.9 Cyclic voltammograms of TyrE-GNEE (Solid line) and GNEE (Dotted line) 0.1M PBS, pH 6.5. Scan Rate 50 mV/s.

Tyrosinase catalyzes the oxidation of phenol group to *o*-quinone, thus allowing a variety of phenolic compounds to be used as substrates of this enzyme. It is well known that this enzyme presents broad substrate specificity. In order to determine the selectivity of the sensor, the voltammetric response of this sensor to other phenolic compounds including L-dopa, dopamine, catechol and phenol was checked. These phenolic compounds actually show no current at −0.100 V, suggesting that there is no interference in the

presence of these substrates. Therefore, it is reasonable that this sensor may be used to selectively detect catecholamines without interference.

Integrity of immobilized tyrosinase construction and its ability to exchange electrons with gold surface allow to observed reduction peak which was attributed to the direct reduction of quinone liberated from the enzyme. When the tyrosinase was absorbed on the surface it was strongly bound to gold nanoparticles and this decreased the ability of nanoparticles transferring electron. The difference of cyclic voltammograms between unmodified electrodes and GNEEs tyrosinase electrode illustrates that tyrosinase has been immobilized successfully.

Figure 3.10 shows the cyclic voltammograms of the enzyme electrode in blank buffer solution (a) and also in buffer solution containing 1 x10^{-4} M catechol (b). In the absence of catechol, only the background current was observed. In contrast, the reduction current increased after catechol was added to the buffer solution. Such an increase in reduction current corresponds to the reduction of quinone species produced by catalytic reaction on the enzyme electrode.

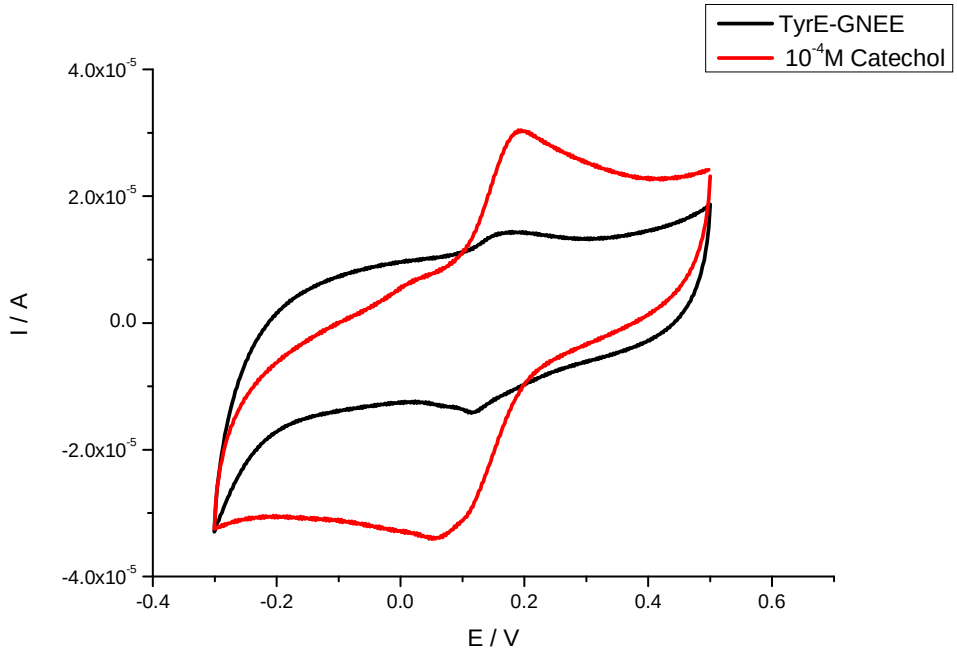

Figure 3.10 Cyclic voltammograms of the enzyme electrode in 0.1M PBS (pH 6.5) without (a) and with 1 x10^{-4} M catechol (b). Potential scan range covers from -200 to 500 mV.

The reduction current is due to the reduction of quinone species liberated from the enzymatic reaction catalyzed by the tyrosinase on the enzyme electrode. The appearance of reduction current indicates that tyrosinase has been successfully immobilized on the electrode surface, and retains its biological activity on the gold.

3.5 Optimization of FIA parameters

Studies were performed using FIA with amperometric detection to improve the analytical performance of the TyrE-GNEEs used for catecholamines studies. The FIA system used in the determination of the L-dopa, dopamine, catechol and phenol was optimized using the univariant method to improve the performance of analysis. Univariant method is one of the most common methods used for optimization, in which one variable at a time is changed and other values around that previously selected or fixed as constant.

3.6 Optimization of detection potential for FIA

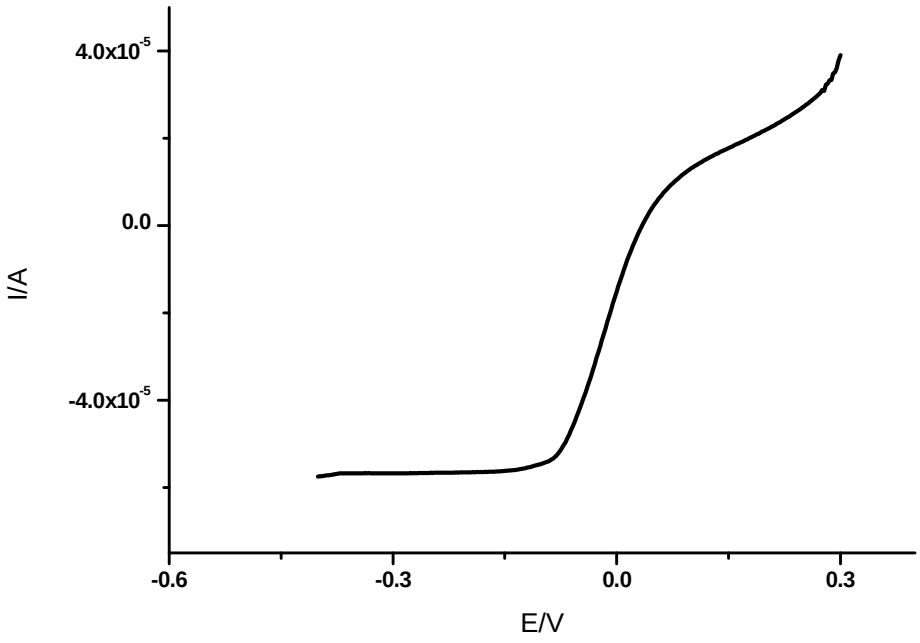

Figure 3.11 Hydrodynamic voltammogram of L-dopa on GNEE at PBS, pH 6.5, scan rate 50 mV/s.

The working electrode TyrE-GNEE was operated at a desired potential and the transient currents were allowed to decay to a steady-state value. At a selected working potential from 0.300 to -0.400 V, the hydrodynamic voltammogram with GNEE (Fig.3.11) revealed a well-defined cathodic voltammetric wave. The steady state current response was obtained at -0.100 mV. The optimal reduction potential of enzyme product at -0.100 mV was therefore selected for flow injection analysis.

3.7 Optimization flow rate for FIA

Optimization of flow rate was also an important parameter of electrochemical detection. The effect of the flow rate on catacholamines determination was studied between 0.5 and 1.6 mL/min (Fig. 3.12). The results show that a flow rate of over 1 mL/min at the entry to the detector was unsuitable because of a large build-up of pressure in the system; however, lower flow rates were associated with lower sampling rates. Therefore, 1 mL/min was set as the optimal value for further studies.

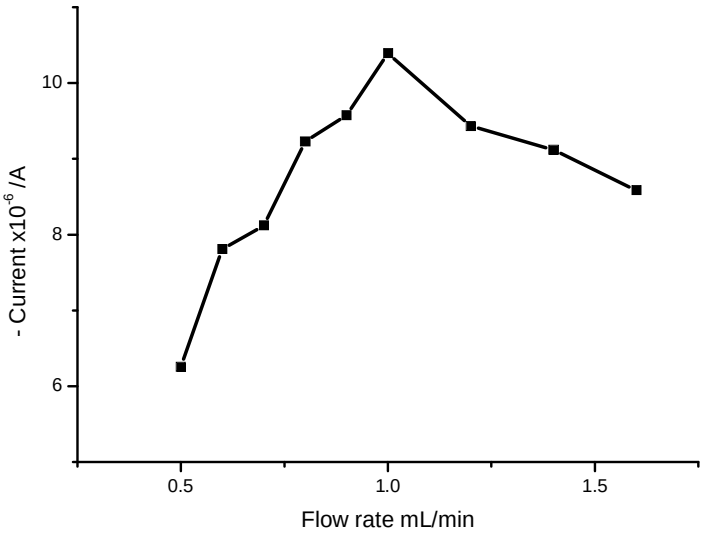

Figure 3.12 Effect of the flow rate on the oxidation of L-dopa on GNEE in 0.1 M at PBS, pH 6.5 at constant potential -0.100 V.

3.8 Analytical calibration

Linear calibration graphs of peak heights of the standards versus the concentration of the standards were plotted by analyzing a known concentration of L-dopa, dopamine, catechol and phenol in the range 10^{-3} to 10^{-6} M. The resulting current was directly proportional to the concentration of the oxidizable species. The plotted points represent the means of at least five independent replicates per standard. The calibration plot demonstrated the relationship between the detector response and the analyte concentration. Measurements were made repeatedly to evaluate the reproducibility of the GNEEs.

Linear calibration graphs of peak heights of the standards versus the concentration of the standards were plotted by analyzing a known concentration of catecholamines in the range from 10^{-6} to 10^{-3} M. The selected concentration range of L-dopa and dopamine falls is within the therapeutic range. The resulting reduction current was directly proportional to the concentration enzyme produced quinones. The plotted points represent the means of at least five independent replicates per standard. The calibration plot demonstrated a linear relationship between the detector response and the analyte concentration and intercepts close to the origin (Figs. 3.14, 3.16, 3.18, 3.20). Under optimized conditions, high reproducible results were obtained, linear calibration was achieved in the $1x10^{-6}$ M to $1x10^{-3}$ M concentration range and the detection limit was $1x10^{-8}$ M. Measurements were made repeatedly to evaluate the reproducibility of the TyrE-GNEE. The results revealed that the electrode had a highly reproducible surface. The limit of detection (LOD) was defined as the lowest concentration of catecholamine that produced a signal that was three times greater than the standard deviation of the current in the absence of analyte under otherwise identical conditions.

3.8.1 Calibration plot for L-dopa

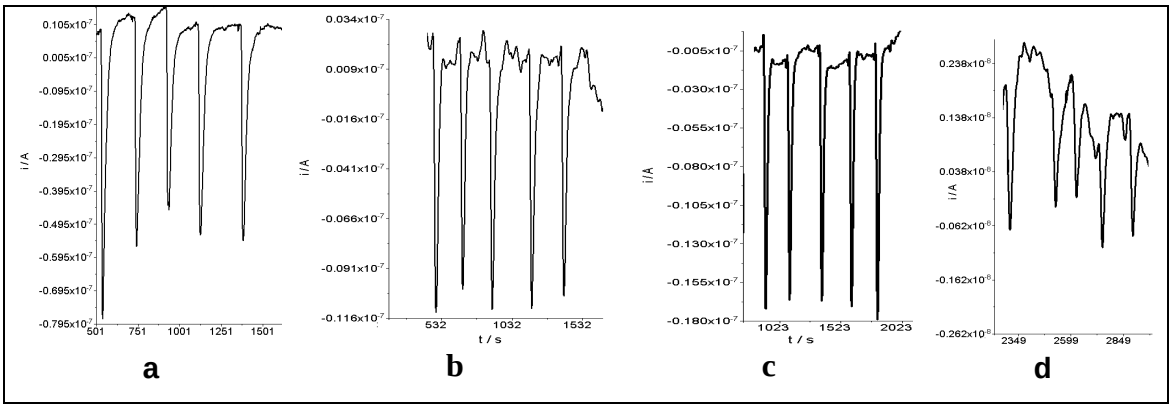

Figure 3.13 FIA responses of L-dopa (a) 10^{-3}, (b)10^{-4}, (c) 10^{-5} and (d) 10^{-6} M in 0.1 M PBS pH 6.5 at -0.100 V vs Ag/AgCl for five continuous injections.

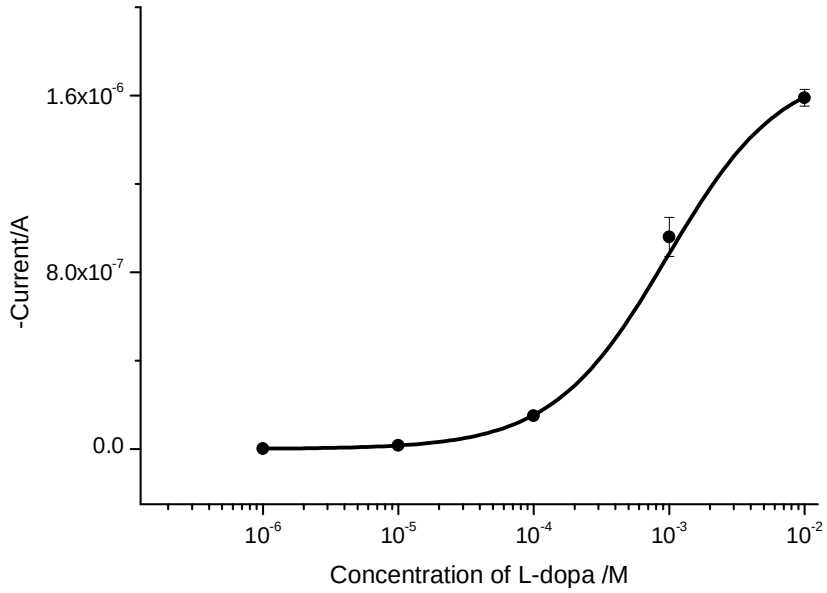

Equation	y = START + (END - START) * x^n / (k^n + x^n)		
Adj. R-Square	0.99825	Value	Standard Error
START		2.73E-10	3.35E-10
END		1.74E-06	5.99E-08
k		9.66E-04	1.45E-04
n		1.02765	0.0386
Limit of detection		$1x10^{-8}$ M	

Figure 3.14 Calibration plot and curve fitting equation for L-dopa under optimized conditions

3.8.2 Calibration plot for dopamine

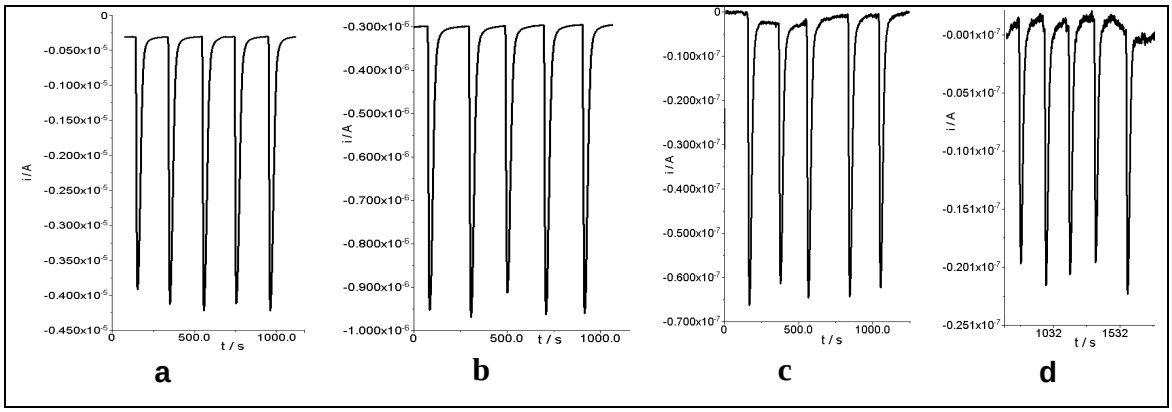

Figure 3.15 FIA responses of dopamine (a) 10^{-3}, (b) 10^{-4}, (c) 10^{-5} and (d) 10^{-6} M in 0.1 M PBS pH 6.5 at -0.100 V vs Ag/AgCl for five continuous injections.

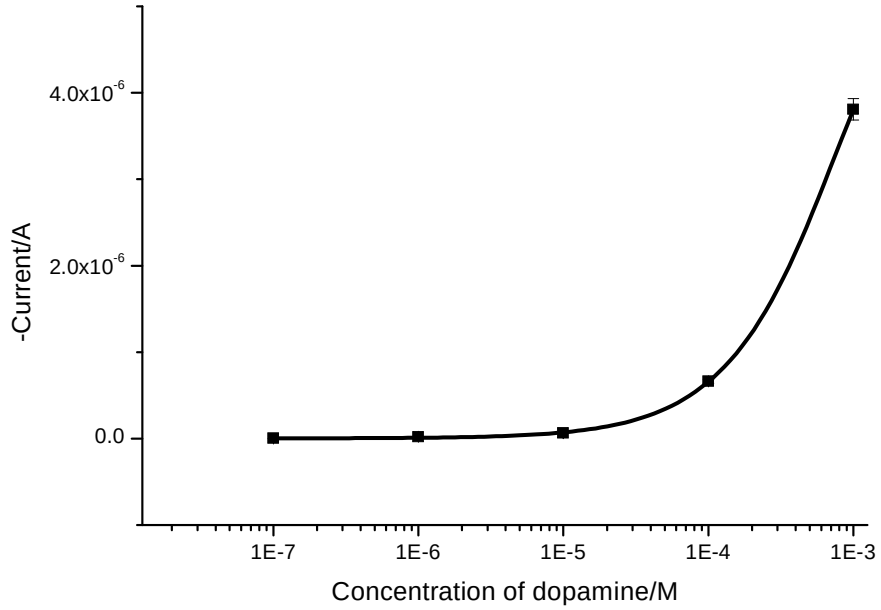

Equation	y = A1*exp(-x/t1) + y0		
Adj. R-Square	0.836	Value	Standard Error
y0		5.08E-06	3.64E-06
A1		-5.08E-06	3.64E-06
t1		7.24E-04	6.35E-04
Limit of detection		$1x10^{-8}$ M	

Figure 3.16 Calibration plot and curve fitting equation for dopamine under optimized conditions

3.8.3 Calibration plot for catechol

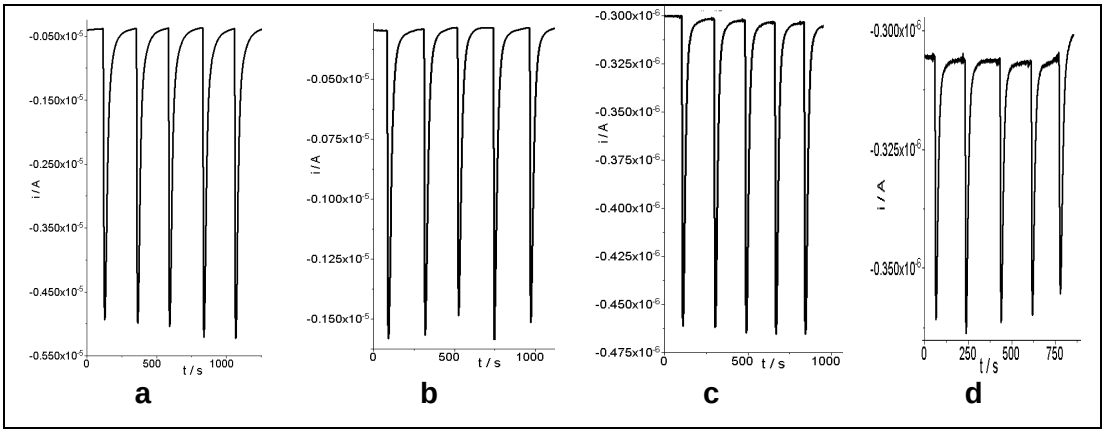

Figure 3.17 FIA responses of catechol (a) 10^{-3}, (b)10^{-4}, (c) 10^{-5} and (d) 10^{-6} M in 0.1 M PBS pH 6.5 at -0.100 V vs Ag/AgCl for five continuous injections.

.

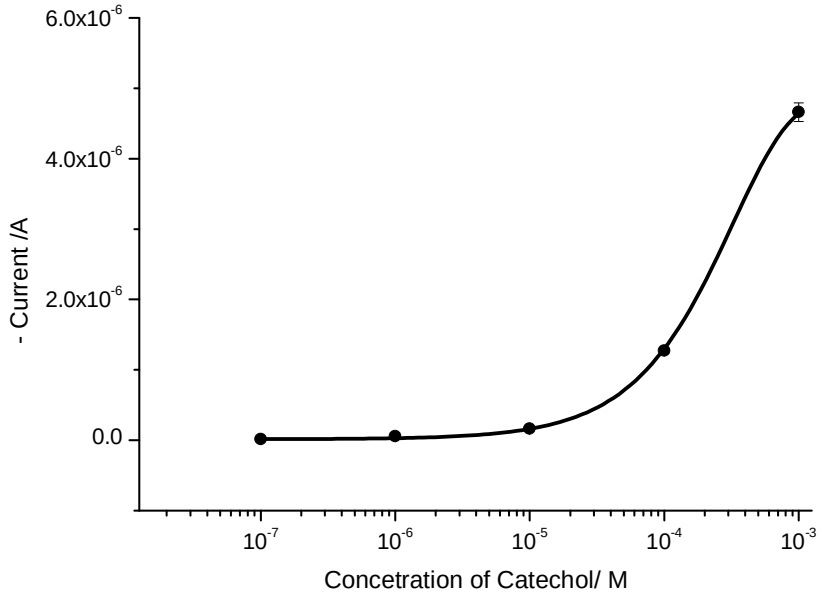

Equation	y = A1*exp(-x/t1) + y0		
Adj. R-Square	0.990	Value	Standard Error
y0		4.87E-06	1.15E-06
A1		-4.85E-06	1.15E-06
t1		3.25E-04	8.14E-05
Limit of detection		$1x10^{-8}$ M	

Figure 3.18 Calibration plot and curve fitting equation for catechol under optimized conditions

3.8.4 Calibration plot for phenol

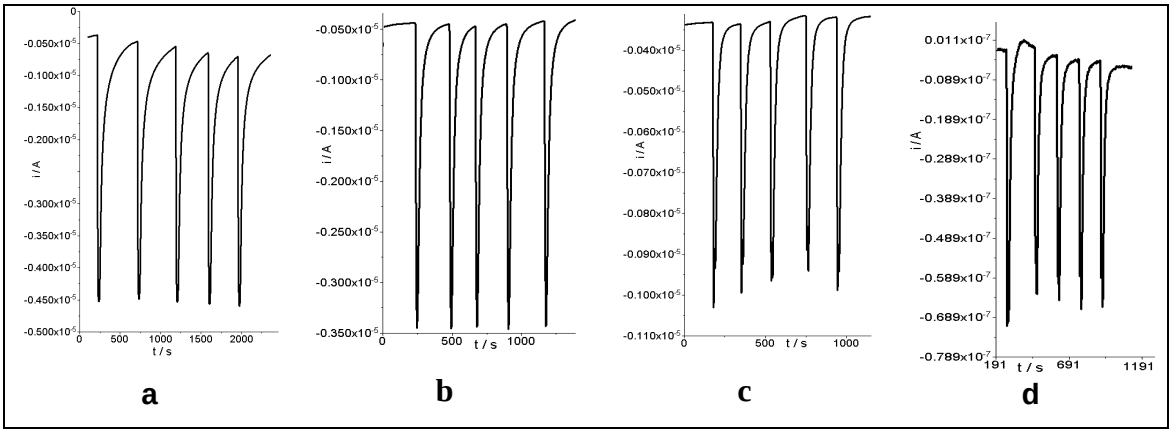

Figure 3.19 FIA responses of phenol (a) 10^{-3}, (b)10^{-4}, (c) 10^{-5} and (d) 10^{-6} M in 0.1 M PBS ph 6.5 at -0.100 V vs Ag/AgCl for five continuous injections.

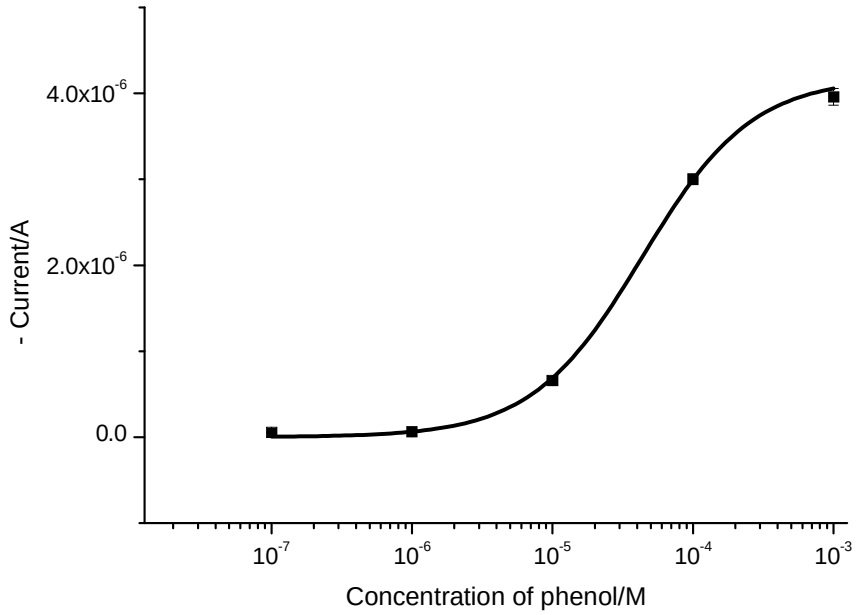

Equation	y=Vmax*x^n/(k^n+x^n)		
Adj. R-Square	0.994	Value	Standard Error
k		4.33E-05	2.24E-05
n		1.10722	0.15811
Limit of detection		$1x10^{-8}$ M	

Figure 3.20 Calibration plot and curve fitting equation for phenol under optimized conditions

3.9 Stability of TyrE-GNEE

The stability of the TyrE-GNEE is very important during the chronoamperometric experiments. It was studied using the same conditions as was above mentioned. For each different addition of 10^{-6} M catechol solution a response time of about 10 s was observed and thereafter a good stability is maintained at TyrE-GNEE during 10 minutes, operating at a potential of -0.1 V, the electrodes being stable for more than a month stored at 4ºC.

3.10 Interference studies

The effect of some possible interfering substances on the TyrE-GNEE biosensor has been investigated. Glucose, ascorbic acid and urea are known to hinder electrochemical measurements at this potential used to monitor the quinone produced in the enzymatic reaction. The results were given in Tables 3.2; 3.3; 3.4; 3.5. Interference studies were revealed that the TyrE-GNEE was good selectivity and sensitivity.

L-dopa and dopamine is clinically very important chemical. So the inference from physiological serum is also very important. Medical grade physiological serum was used in this study. Calculated amount of L-dopa and dopamine were spiked with serum and analyzed using TryE-GNEE. The percentage of recovery was calculated from FIA responses of L-dopa and dopamine and 83% and 87% recovery was observed for L-dopa and dopamine, respectively. The results were shown in Figs.3.21; 3.22.

Table 3.2 FIA responses of L-dopa with interference 20mM ascorbic acid, 100mM glucose and 100mM urea in 0.1M PBS pH6.5 at -0.1V vs Ag/AgCl.

L-dopa/ M	FIA responses for L-dopa with interferences, –current/A (n=5)			
	Standard	With ascorbic acid	With glucose	With Urea
10^{-6}	1.75E-09	1.50E-09	2.18E-09	1.15E-09
10^{-5}	1.62E-08	1.40E-08	1.97E-08	1.10E-08
10^{-4}	1.50E-07	1.24E-07	1.64E-07	1.14E-07
10^{-3}	9.60E-07	8.59E-07	8.16E-07	6.76E-07

Table 3.3 FIA responses of dopamine with interference 20mM ascorbic acid, 100mM glucose and 100mM urea in 0.1M PBS pH6.5 at -0.1V vs Ag/AgCl.

Dopamine / M	FIA responses for dopamine with interferences, –current/A (n=5)			
	Standard	With ascorbic acid	With glucose	With Urea
10^{-6}	2.17E-08	1.83E-08	1.89E-08	1.54E-08
10^{-5}	6.24E-08	5.94E-08	6.46E-08	7.05E-08
10^{-4}	6.62E-07	6.39E-07	6.85E-07	5.55E-07
10^{-3}	3.81E-06	3.96E-06	3.33E-06	2.19E-06

Table 3.4 FIA responses of catechol with interference 20mM ascorbic acid, 100mM glucose and 100mM urea in 0.1M PBS pH6.5 at -0.1V vs Ag/AgCl.

Catechol/M	FIA responses for catechol with interferences -Current/A (n=5)			
	Standard	With ascorbic acid	With glucose	With Urea
10^{-6}	5.46E-08	5.24E-08	5.11E-08	4.89E-08
10^{-5}	1.61E-07	1.87E-07	1.66E-07	1.35E-07
10^{-4}	1.27E-06	1.52E-06	1.88E-06	1.13E-06
10^{-3}	4.66E-06	5.68E-06	5.22E-06	4.58E-06

Table 3.5 FIA responses of phenol with interference 20mM ascorbic acid, 100mM glucose and 100mM urea in 0.1M PBS pH6.5 at -0.1V vs Ag/AgCl.

Phenol/M	FIA responses for phenol with interferences -Current/A (n=5)			
	Standard	With ascorbic acid	With glucose	With Urea
10^{-6}	6.18E-08	6.63E-08	6.92E-08	6.52E-08
10^{-5}	6.58E-07	6.13E-07	6.92E-07	6.52E-07
10^{-4}	3.00E-06	2.06E-06	2.37E-06	2.90E-06
10^{-3}	3.96E-06	4.50E-06	4.80E-06	3.87E-06

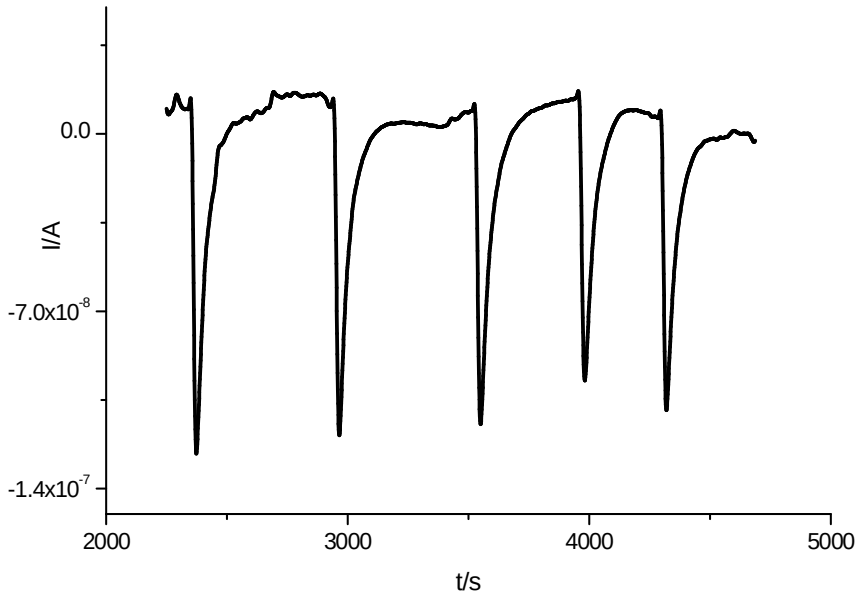

Figure 3.21 FIA responses of L-dopa 10^{-4} M spiked in serum samples in 0.1 M PBS, pH 6.5 at -0.100 V vs Ag/AgCl for five continuous injections, 83% recovery was observed.

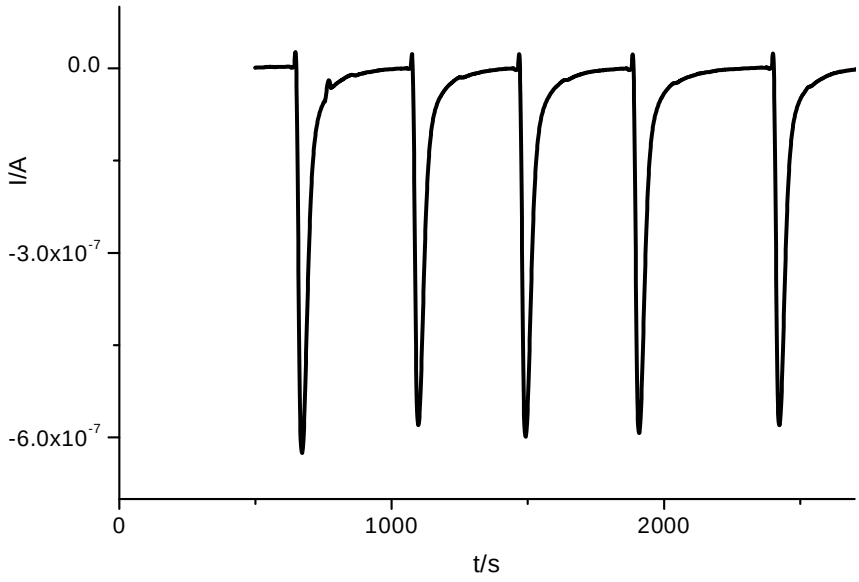

Figure 3.22 FIA responses of Dopamine 10^{-4} M spiked in serum samples in 0.1 M PBS, pH 6.5 at -0.100 V vs Ag/AgCl for five continuous injections, 87% recovery was observed.

4. Conclusions

- In conclusion, gold nanoelectrode ensembles (GNEEs), 50 nm in diameter and 180 nm in length were prepared by electroless template synthesis in polycarbonate filter membranes, followed by selective controlled sequential polycarbonate dissolution using DCM/EtOH (V∶V＝1∶3).
- The morphology of the nanowires and cylindrical GNEEs was imaged by scanning electron microscopy. The protruding nanoelectrodes were in good parallel order. EDX study showed that the nanoelectrode elements consisted of pure gold.
- The electrochemical evaluation of the 3D electrodes was conducted using the well known $[Fe(CN)_6]^{3-}/[Fe(CN)_6]^{4-}$ couple.Compared with 2D disc GNEEs, the 3D GNEEs significantly enhanced the current response in cyclic voltammetry. The linear relationship with a slope of 0.5 between log I_{pc} and log v shows that linear diffusion is dominant on the 3D GNEEs at conventional scan rates. The electrochemical results demonstrated the fact that electron transfer process could be effectively improved at the 3D cylindrical GNEEs. Linear diffusion is dominant on the cylindrical GNEEs at conventional scan rates.
- In summary, the experiments described above illustrate an attractive construction of renewable biosensors for the catecholamines detection. Tyrosinase maintains its enzymatic properties on the 3D GNEE surface. In this work, we prepared TyrE-GNEE that shows better electrochemical properties than conventional Au electrode.
- Biosensors based on this nanostructure have improved analytical performances compared to the conventional electrode. Specifically, the biosensor shows a wider linear response to catecholamines in the range from 10^{-6} to 10^{-3} M and a higher maximum current density.
- Negligible or less interferences from species like glucose, ascorbic acid and urea were observed at a potential of -0.100 V (vs. Ag/AgCl). This sensor was successfully applied to the determination of L-dopa and dopamine spiked in serum samples.
- The above facts indicate that the gold nanoelectrodes can be also used in the fabrication of other biosensors based on oxidases, such as biosensors for choline, cholesterol, and alcohol.

5. Bibliography

1. Stoica L., Lindgren-Sjőlander A., Ruzgas T., Gorton L., *Analytical Chemistry,* 76 (2004) 4690

2. Wightman R.M., May L.L., Michael A.C., *Analytical Chemistry.* 60 (1988) 769A

3. Peters J.L., Yang H., Michael A.C., *Analytical Chimica Acta,* 412 (2000)1

4. Vinton B.J., Wightman R.M., *Analytical Chemistry.* 75 (2003) 414A

5. Lowe, C. R. Biosensors. *Trends in Biotechnology* 2 (1984) 59

6. Chaubey, A.; Malhotra, B.D, *Biosensors and Bioelectronics,* 17 (2002) 441

7. Eggins, B.; *Chemical sensors and biosensors*. Analytical Techniques in the Sciences. John Wiley & Sons, West Sussex, (2002)

8. Kasemo, B. *Surface Science 500* (2002) 656

9. Chen, J.; Miao. Y.; He, N.; Wu, X.; Li, S.; *Biotechnology Advances,* 22 (2004) 505

10. Zhang W., Li G., *Analytical Science, 20* (2004) 603

11. Newman J.; Setford. S., *Molecular Biotechnology,* 32 (2006) 249

12. Choi M., Panga W. , D Xiaob., Wu X.. *Analyst* 126 (2001) 1558

13. El-Sayed IH, Huang XH, El-Sayed MA. *Nano Letters, 5* (2005) 829

14. Tsekenis G., Garifallou G., Davis F., Millner P., Gibson T., Higson. S., *Analytical Chemistry,* 80 (2008) 2058

15. Ricci F., Volpe G., Micheli L., Palleschi G., Analytical *Chimica Acta*, 605 (2007) 111

16. Mehrvar M., Abdi M., *Analytical Science, 20* (2004) 1113

17. Tombelli S., Minunni M., Mascini M., *Biomolecular Engineering, 24* (2007) 191

18. Strehlitz B., Nikolaus N., Stoltenburg R., *Sensors 8* (2008) 4296

19. DeAngelis K., Firestone M. , Lindow. S., Appl*. Environmental Microbiology,* 73 *(*2007) 3724.

20. Ahmed, M. U., Hossain, M. M., Tamiyaa, E., *Electroanalysis,* 20 (2008) 616

21. Liu Y., Yuan R., Chai Y.Q., Tang D.P., Dai J.Y., Zhong X., *Sensors and Actuators B: Chemical*, 115 (2006) 109

22. Bakker E., *Analytical Chemistry,* 76 (2004) 3285

23. Wang J., *Analyst 130* (2005) 421

24. Chaubey A., Malhotra B.D., *Biosensors and Bioelectronics, 17* (2002) 441

25. Patel, P. D. *Trends Analytical Chemistry,* 21 (2002) 96

26. Shkotova V., Goriushkina T.B., Tran-Minh C., Chovelon J.-M., Soldatkin A.P., Dzyadevych S.V., *Materials Science Engineering, C* 28 (2008) 943

27. Ohnuki H,, Saiki T,, Kusakari A, Endo H,, Ichihara M, Izumi M, *Langmuir 23* (2007) 4675

28. Marzouk S.A., Ashraf S.S., Tayyari K.A., *Analytical Chemistry*, 79 (2007) 1668

29. Mello L.D., Kubota L.T., *Food Chemistry,* 77 (2002) 237

30. Liu Y., Yuan R., Chai Y.Q., Tang D.P., Dai J.Y., Zhong X., *Sensors and Actuators B: Chemical,* 115 (2006) 109

31. Yuqing M., Jianquo G., Jianrong C., *Biotechnology Advances, 21* (2003) 527

32. Pohanka M., Jun D., Kuča K., *Drug Chemical Toxicology*, 30 (2007) 253

33. Davis F., Hughes M.A., Cossins A.R., Higson S.P., *Analytical Chemistry*, 79 (2007) 1153

34. Ouerghi O., Touhami A., Jaffrezic-Renault N., Martelet C., Ouada H.B., Cosnier S., *Bioelectrochemistry*, 56 (2002) 131

35. Clark L. C., Lyons C., *Annals of New York Academy Sciences*, 102 (1962) 29

36. Updike S. J., Hicks G. P., *Nature 214* (1967) 986

37. Guilbault G. G., Lubrano G. J., Analytical *Chimica Acta*, 64 (1972) 439

38. Feldman B., McGarraugh G., Heller A., Bohannon N., Skyler J., DeLeeuw E., Clarke D., Freestyle(TM), *Diabetes Technology and Therapeutics, 2* (2000) 221

39. Husain M., Husain Q., *Environmental Science & Technology, 38* (2008) 1

40. Gregg B. A., Heller A., *Analytical Chemistry, 62* (1990) 258

41. Gregg B. A., Heller A., J*ournal of Physical Chemistry,* 95 (1991) 5970

42. Singh M., Verma N., Garg A. K., Redhu N., *Sensors and Actuators B:Chemical. 134* (2008) 34

43. Nunes G. S., Marty J. L., Immobilization of Enzymes and Cells: Immobilization of Enzymes on Electrodes, *Methods in Biotechnology*, 2006, Vol. 22, 239-250

44. Gorton L.; *Journal of Electroanalytical Chemistry,* 7 (1995) 23

45. Liu Y., Yuan R., Chai Y.Q., Tang D.P., Dai J.Y., Zhong X., *Sensors and Actuators B: Chemical, 115* (2006) 109.

46. Wightman R.M., *Science 240* (1988) 415.

47. Thevenot D.R., Toth K., Durst R.A., Wilson G.S., *Biosensors and Bioelectron*ics, 16 (2001) 121

48. Wang J., Pedrero M., Sakslund H., Hammerich O., Pingarron J., *Analyst*, 121 (1996) 345

49. Skladal P., Kalab T., *Analytical Chimica Acta*, 316 (1995) 73

50. Deng A.P., Yang H., *Sensors and Actuators B: Chemical*, 124 (2007) 202

51. Vo-Dinh T., Cullum B.M., Stokes D.L., *Sensors and Actuators B:Chemical*, 74 (2001) 2

52. Haruyama T., *Advanced Drug Delivery Reviews*, 55 (2003) 393

53. Jain KK., *Expert Reviews Molecular Diagnostics, 3* (2003) 15

54. Niemeyer C. M., *Angewandte Chemie International, Ed. 40* (2001) 4129

55. Wang J., *Analyst*, 130 (2005) 421

56. Gooding J.J., Wibowo R., Liu J.Q., Yang W., Losic D., Orbons S., Mearns

F.J.,Shapter J.G., Hibbert D.B., *Journal American Chemical Society, 125* (2003) 9006

57. Yu X., Chattopadhyay D, Galeska I., Papadimitrakopoulos F., Rusling J.F. *Electrochemistry Communications*,5 (2003) 408.

58. Patolsky F., Weizmann Y., Willner I. *Angewandte Chemie International,* Ed. 43 (2004) 2113

59. Marc D., Sophie D.C., *Biosensors and Bioelectronics* 18 (2003) 943

60. Miao Y., Qi M., Zhan S., He N., Wang J., Yuan C., Analytical Letters, 32 (1999) 1287

61. Nirmal M., Norris D.J., Kuno M., Bawendi M.G., Efros A.L., Rosen M*., Physical Review Letters* 75 (1995) 3728

62. Manna L., Scher E.C., Alivisatos. A.P., *Journal of Cluster Science,* 13 (2002) 521

63. Alivisatos A.P., *Science*, 271 (1996) 933

64. Lieber C.M., *Solid State Communications,* 107 (1998) 607

65. Albe V., Jouanin C., Bertho D., Journal *of Crystal Growth*, 185 (1998) 388

66. Smalley R.E., Yakobson B.I., *Solid State Communications, 107* (1998) 597

67. Williamson A.J., Zunger A., *Physical Review B: Condensed Matter*, 59 (1999) 15819

68. Bruchez M, Moronne M., Gin P., Weiss S., Alivisatos. A.P., *Science 281* (1998) 2013

69. Alivisatos A.P., *Journal Physical Chemistry,* 100 (1996) 13226

70. Jianrong C., Yuqing M., Nongyue H., Xiaohua W, Sijiao L., *Biotechnology Advances 22* (2001) 505

71. Shi H., Yeh J.I. , Part I., *Nanomedicine,* 2 (2007) 587

72. Shi H., Xia T., Nel A.E., Yeh J.I., *Nanomedicine, 2* (2007) 599

73. Ulman, A., *Chemical Reviews*, 96 (1996) 1533

74. Schwartz D. K., Annual *Review of Physical Chemistry* 52 (2001) 107

75. Gooding J.J., *Electrochemistry Communications,* 1 (1999) 119

76. Radi A.E., Sanchez J.L.A., *Analytical Chemistry, 77* (2005) 6320

77. Rodgers P.J., Shigeru A., *Analytical Chemistry,* 77 (2007) 9276

78. Raj C.R., Ohsaka T., *Electroanalysis, 14* (2002) 679

79. Yang, N., Wang, X., *Colloids and Surfaces B, 61*(2008) 277

80. Zhao W., Xu J.J., Chen H.Y., *Electroanalysis* 18 (2006) 1737

81. Gaspar S., Zimmermann H., Gazaryan I., Csˆregi E., Schuhmann W., *Electroanalysis*, 13 (2001) 284.

82. Gooding J. J., Hibbert D. B, Trends *Analytical Chemistry*, 18 (1999) 525.

83. Ferreti S., Paynter S., Russel D. A., Sapsford K. E., *Trends Analytical Chemistry*, 19 (2000) 530.

84. Campuzano S., Galvez R., Pedrero M., F. J., M. de Villena Pingarron J. M*., Journal Electroanalytical Chemistry, 526* (2002) 92

85. Dalmia A., Liu C.C., Savinell, R.F., *Journal Electroanalytical Chemistry, 430* (1997) 205

86. Esplndiu M.J., Hagenstrom H., Kolb D.M., *Langmuir* 17(2001) 828

87. Uosaki K., Sato Y., Kita H., *Langmuir 7* (1991) 1510

88. Bharathi S., *Anaytical Communications*. 35 (1998) 29

89. Bharathi S., Nogami M., Lev O., *Langmuir 17* (2001) 2602

90. Jia J., Wang B., Wu A., Cheng G., Li Z., Dong S., *Analytical Chemistry*, 74 (2002) 221

91. Ducey M. W., Meyerhoff M. E., *Electroanalysis* 10 (1998)157

92. Padeste C., Kossek S., Lehmann H. W., Musil C. R., Gobrecht J., Tiefenauer L., *Journal Electrochemical Society,*143 (1996) 3890.

93. Brunetti B., Ugo P., Moretto L. M., Martin C. R., *Journal of Electroanalytical Chemistry* 491(2000) 166.

94. Pingarron J.M., Yanez-Sedeno P., Gonzalez-Cortes A*., Electrochimica Acta* 53,

(2008) 5848.

95. Shulga, O., Kirchhoff J. R., *Electrochemistry Communications,* 9 (2007) 935

96. Liu, S. Q., Ju, H. X., *Biosensors and Bioelectronics,* 19 (2003) 177

97. Liu S. Q., Yu J. H., Ju H. X. *Journal of Electroanalytical Chemistry,* 540 (2003) 61

98. Liu S. Q., Ju, H. X. *Analytical Biochemistry, 307* (2002) 110

99. Zhang S. X., Wang, N., Yu H. J., Niu, Y. M. , Sun, C. Q., *Bioelectrochemistry*, 67 (2005) 15

100. Luo X. L., Xu J. J., Du Y., Chen H. Y. *Analytical Biochemistry, 334* (2004) 284.

101. Luo X. L., Xu J. J., Zhang Q., Yang G. J., Chen H. Y., *Biosensors and Bioelectronics 21* (2005) 190

102. Manso J., Mena M. L., Yanez-Sedeno P., Pingarron J. M., *Journal of Electroanalytical Chemistry* 603 (2007)1

103. Njagi, J., Andreescu, S., Biosensors *and Bioelectronics,* 23 (2007) 168

104. Possin G.E., *Review of Scientific Instrum*ents, 41 (1970) 772

105. Martin C.R., *Science* 266 (1994) 1961

106. Yeh J.I., Zimmt M.B., Zimmerman A.L., *Biosensors and Bioelectronics,* 21 (2005) 973

107. Roberts M.A., Kelley S.O., *Journal of the Am*erican *Chemical Society,* 129 (2007) 11356

108. Yeh J.I., Lazareck A., Kim J.H., Xu J., Du S., *Biosensors and Bioelectronics, 23* (2007) 568

109. Lerch K., Longoni C., Jordi, E., *Journal of Biological Chemistry,* 257 (1982) 6408

110. Rûzicka, J.; Hansen, E.H.; Flow Injection Analysis; (1981) *Wiley eds.,* NY

111. Karlberg, B., and Pacey, G.E., Flow Injection Analysis, a pratical guide, *Elsevier Science Publishers B.V*., Amesterdam (1989)

112. Lerch K., Longoni C., Jordi, E., *Journal of Biological Chemistry,* 257 (1982) 6408

113. Huber M., Hintermann G., Lerch, K., *Biochemistry* 24 (1985) 6038

114. Mayer A. M., *Phytochemistry*, 26 (1986) 11

115. Kwon B. S., Haq A. K., Pomerantz S. H., Halaban R, *Proceddings National Academy of Sciences U.S.A.,* 84 (1987)7473

116. Retama J.R., López M.S.P., Pérez J.P.H., Cabanillas G.F., Cabarcos E.L, Ruiz B.L., *Biosensors and Bioelectronics,* 20 (2005) 2268

117. Pita M.T.P., Reviejo A.J., F.J.M. de Villena, Pingarrón J.M., *Analytical Chimica Acta*, 340 (1997) 89

118. Jolley R. L., Evans L. H., Makino N. , Mason H. S., *Journal of Biological Chemistry,* 249 (1974) 335

119. Pomerantz S. H., Warner M. C*., Journal of Biological Chemistry,* 242 (1967) 5308

120. Naish S., Riley P. A., *Biochemical Pharmacology,* 38 (1989) 1103

121. Min K., Yoo Y.J., *Talanta 80* (2009) 1007

122. Ozoner S. K., Yalvac M., Erhan E., *Current Applied Physics 10* (2010) 323

123. Rivas G., Solis V., *Analytical Chemistry, 63* (1991) 2762

124. Mannino S., Cosio M., *Analyst* 119 (1994) 2001

125. Wang J., Chen L., *Analytical Chemistry, 67* (1995) 3824

126. Xiaoya H., Zongzhou L., *Analyst 120* (1995) 1555

127. Dennison M., Hall J., Turner A., *Analitical Chemistry, 67* (1995) 3922

128. Kiba N., Suzuki H., Furusawa M., *Talanta 40* (1993) 995

129. McArdle F. A., Persaud K. C., *Analyst*, 118 (1993) 419

130. Besombes J. L., Cosnier S., Labbe P., Reverdy G., *Analytical Chimica Acta*, 311 (1995) 255

131. Vedrine C., Fabiano S., Tran-Minh C., *Talanta*, 59 (2003) 535

132. Wang J., Nascimento V. B., Kane S. A, Rogers K., Smyth M. R., Angnes L., *Talanta*, 43 (1993) 1903

133. Pedano L., Rivas G.A., *Talanta* 53 (2000) 489

134. Rogers K.R., Becker J.Y., Cembrano J., Chough S.H, *Talanta* 54 (2001) 1059

135. Ortega F., Domínguez E., Burestedt E., Emnéus J., Gorton L., Varga G.M., Journal of *Chromatography, A* 675 (1994) 65.

136. Campuzano S., Pedrero B.S.M., F.J.M. de Villena, Pingarrón J.M., *Analytical Chimimica Acta,* 494 (2003) 187

137. Notsu H., Tatsuma T., *Journal of Electroanalytical Chemistry,* 566 (2004) 379

138. Xue H., Shen Z., *Talanta* 57 (2002) 289

139. Naish S., Cooksey C. J., Riley P. A., *Pigment Cell Research,* 1(1988) 379

140. Schoot-Uiterkamp A. J. M., Mason H. S., *Proceedings. National Academy of Sciences U.S.A., 70*, (1973) 993

141. Nishioka, K., Eur. *Journal of Biochemistry,* 85 (1978) 137

142. Delvaux, S. Demoustier-Champagne, *Biosensers and Bioelectronics*, 2003, 18, 943.

X